NIOBIUM NANOWIRE YARNS AND THEIR APPLICATION AS ARTIFICIAL MUSCLE

by

SEYED MOHAMMAD MIRVAKILI

B.A.Sc., University of British Columbia, Canada, 2011

A THESIS SUBMITED IN PARTIAL FULFILLMENT OF

THE REQUIREMENTS FOR THE DEGREE OF

MASTER OF APPLIED SCIENCE

in

THE FACULTY OF GRADUATE STUDIES

(Electrical and Computer Engineering)

THE UNIVERSITY OF BRITISH COLUMBIA

(Vancouver)

April 2013

ABSTRACT

Since the discovery of carbon nanotubes, various devices have been made in different fields of science and engineering. The mechanical and electrical properties that carbon nanotubes offer make them a great candidate for use in the structure of artificial muscles. In this thesis, for the first time, we have demonstrated that metallic nanowires can be engineered to become strong and comparable to the CNT yarns in mechanical and electrical properties. The niobium yarns offer conductivity of up to 3×10^6 S m^{-1}, tensile strength of up to 1.1 GPa and Young's modulus of 19 GPa. The niobium nanowire fibres are fabricated by extracting the niobium nanowires from copper-niobium nano-composite matrix, which was made by using a severe plastic deformation process. As a practical application, torsional artificial muscles were made out of the niobium yarns by twisting and impregnating them with paraffin wax. Upon applying voltage to the twisted yarn the wax melts and expands due to the heat generated by the current. Thermal expansion of wax untwists the yarn, which translated to torsional actuation. Torsional speeds of 7,200 RPM (in a destructive test) and 1,800 RPM (continuous) were achieved. In addition to torsional actuation, niobium yarns also can provide up to 0.24% of isobaric tensile actuation along the yarn's axis at 20 MPa load. Due to the high conductivity of the niobium yarns, the actuator can be made to actuate by even one single 1.5 V battery (for a 1 cm of niobium yarn). The electrochemical capacitance of niobium yarns was measured to be 1.3×10^7 F m^{-3} at a scan rate of 25 mV s^{-1} in 0.2 M TBAPF$_6$ salt dissolved in acetonitrile. This value is comparable to the electrochemical capacitance of the carbon multiwalled nanotube yarns.

PREFACE

A version of chapter 2 – 5 is published in the journal of Advanced Functional Materials (S. M. Mirvakili, A. Pazukha, W. Sikkema, C. W. Sinclair, G. M. Spinks, R. H. Baughman, and J. D. W. Madden, "Niobium Nanowire Yarns and their Application as Artificial Muscles," Advanced Functional Materials, 2013/adfm.201203808). I was the lead investigator and responsible for composition of majority of the manuscript. More details of task divisions are mentioned below:

- **Identification and design of the research program**

  This work is a follow up to the work on torsional carbon multiwalled nanotube artificial muscles initiated by our collaborators in UT Dallas (Dr. Baughman's group). The idea of utilizing niobium nanowire yarns instead of CNT yarns was proposed by Dr. John D. Madden.

- **Performing the research**

  Cu-Nb matrix etching, some electrochemical tests, and EDX measurements were performed by Alexey Pazukha. The Cu-Nb matrix was provided by Dr. Chad W. Sinclair. The rest of the experiments (including some electrochemical tests) were performed by the author.

- **Data analyses**

  The data in this thesis are analyzed by the author and Dr. John D. Madden. I have also benefitted from the comments made by Dr. Ray H. Baughman and Dr. Geoffrey M. Spinks via email.

- **Manuscript preparation**

  All manuscripts included in this thesis are written by the first and principal author.

TABLE OF CONTENTS

LIST OF TABLES

LIST OF FIGURES

ACKNOWLEDGMENT

First and foremost, I would like to express my deepest appreciation to my supervisor Dr. John D. W. Madden for providing me ongoing support, guidance and motivation. John gave me a lot of freedom to explore and conduct research on different projects in the lab and even gave me the opportunity of working on some of my own ideas as side projects. His deep and thoughtful questions taught me to how question and examine every phenomenon that I observe. I owe a particular thanks to him for encouraging me to learn other fields of science and engineering such as biology, mechanics, physics, and chemistry, all of which I am sure will help me in marching across disciplines to find the best solution for real engineering problems.

I would like to thank Natural Science and Engineering Research Council of Canada for supporting this project through an Alexander Graham Bell Canada Graduate Scholarship and a Discovery grant.

I owe special thanks to my family whom without their support; I wouldn't be at the stage I am now. I owe my mother a lot. Her perpetual love, support, and encouragement have always been there for me. Special thanks to my sister for her kind advice throughout my life. Finally and most importantly, I would like to dedicate this thesis to my deceased father, who always gave me the courage and confidence in exploring different fields in my education and most importantly providing me the best possible environment to grow up.

At the end, I would like to thank the following people:

- Dr. Ke Han at National High Field Magnet Laboratory, Florida State University for providing us with Cu-Nb wires.

CHAPTER 1 – Introduction

1.1 Motivation of the study

Many types of artificial muscles have been studied and characterized [1]. Some major drawbacks of the current technologies are either high operating voltage [1] or slow response, and low efficiency. In this study a new type of artificial muscle is developed that operates at low voltages (on the order of volts) and has a quick response to the input signal (on the order of ms). Work has previously been done with carbon multiwalled nanotubes (MWNT), but operating with higher voltages [2]. Although carbon multiwalled nanotube yarns have remarkable mechanical and electrical properties, only few groups in the world can fabricate them. Therefore, finding an abundant alternative material that is more conductive than carbon nanotubes, compliant, and twistable was one of the main motivations of this study.

1.2 Objectives of the study

One of the main purposes of this study was to find the mechanical properties of niobium nanowire yarns and demonstrate a practical application. Achieving niobium yarns with good mechanical properties by engineering the fibres and also demonstrating that the mechanism of torsional actuation works in other conductive materials in addition to carbon multiwalled nanotubes were other two goals for this work.

1.3 Organization of the thesis

The thesis is divided into five chapters.

Chapter 1 Introduction: Motivation and objectives of the study are discussed in this chapter.

Chapter 2 Background: Artificial muscle is defined and different types of artificial muscles are compared in this chapter.

Chapter 3 Materials and Methods: The techniques used to characterize the mechanical and electrical properties of the niobium yarns as well as the methods used to measure the actuation performance are mentioned in this chapter.

Chapter 4 Results and Discussion: The results of the experiments are discussed and justified with some theories. It is shown that the torsional actuation mechanism for carbon multiwalled nanotubes also applies to other materials such as niobium nanowire yarns.

Chapter 5 Conclusions and Recommendations: The conclusion of this work as well as recommendations for future work and some ideas on this work are given in this chapter. The advantages of niobium nanowire yarn and some biomedical applications are also mentioned in this chapter.

Derivation of the formulas used in the main text and also details of the results for some experiments as well as several additional figures are presented in the appendices.

CHAPTER 2 – Background[1]

In this chapter the term 'artificial muscle' is defined and the primary artificial muscle technologies are introduced in four major categories. Mechanical properties of nanofibres and yarns are also discussed. At the end, some applications are mentioned and the interested figures of merit are defined.

2.1 Yarns and their properties

When made sufficiently fine, metallic nanowires (whiskers) are found to be defect free and to have mechanical properties that approach those predicted by the intrinsic bond strength [3]–[8]. The resulting tensile strengths (e.g. ~9 GPa for Cr whiskers) [6] and elongations at break (~5% for Fe whiskers) [3] approach those of the much vaunted carbon nanotube, with carbon multiwalled nanotubes for example demonstrating tensile strengths in the range of 11 to 63 GPa and elongations of 3 to 13% [9]. Such metallic whiskers have been used successfully as reinforcements in nanocomposites. The whiskers can be produced in-situ by phase transformation [10] or through deformation processing [11]–[13] in which nanowhisker reinforced metallic wires are created through a repeated process of 'bundle-drawing'. Copper-niobium wires with tensile strengths of ~2 GPa produced by this method are used as ultra-high strength electrical conductors for high field magnets [14].

It has been demonstrated that twisting carbon multiwalled nanotube yarns makes them stronger while retaining their flexibility and performance [15]. Strengths of up to 300 MPa are measured for single-ply twisted carbon multiwalled nanotubes (460 MPa for two-ply yarns) [15]. Introducing coiling to the yarns (by 'over twisting' the yarns) increases the actuation strain [2], but at the cost of occupying the other two dimensions of space for storing the coil.

It is worth mentioning that the concept of twisting a fibre for the purpose of actuation is not limited to carbon nanotubes and niobium nanowires. Linear and torsional actuations were observed by twisting two strands of hair together and applying heat to them. It is also

---

[1]A version of this chapter is published. S. M. Mirvakili, A. Pazukha, W. Sikkema, C. W. Sinclair, G. M. Spinks, R. H. Baughman, and J. D. W. Madden, "Niobium Nanowire Yarns and their Application as Artificial Muscles," *Advanced Functional Materials*, 2013/adfm.201203808.

demonstrated that a polymer strand can be twisted together with niobium yarn while maintaining and in some cases improving the actuation performance.

2.2 Artificial muscles

'Artificial muscle' is a generic term used for materials or devices that can reversibly contract, expand, or rotate within one body due to an external stimulus (voltage, current, pressure, temperature, etc). There are some artificial muscles that can generate other types of motions, such as bending, by either utilizing more than one of the actuation components (contraction, expansion, and rotation) or making an asymmetry in the actuation axis. For example, by making one side of the muscle contract (or preventing it from moving) while the other side expands, bending can be achieved. Pneumatic linear or rotary actuators have two components (e.g. a shaft and a piston) and the actuation is not occurring within one body; therefore, it may not be called an artificial muscle. Artificial muscles can be divided into four major groups based on their actuation mechanism:

- **Actuation based on applying electric field:** Electroactive polymers (EAPs) such as dielectric elastomer actuators (DEAs), relaxor ferroelectric polymers, and liquid crystal elastomers fall under this category.

- **Actuation based on gas pressure:** Pneumatic artificial muscles (PAMs) operate by a pressurized air filling a pneumatic bladder. Upon applying gas pressure to the bladder, isotropic volume expansion is expected, however the tough braided wires that confines the bladder, translate the volume expansion to a linear contraction along the axis of the actuator (Figure 2.1). McKibben artificial muscle belongs to this category and can only contract or expand upon applying pressure (Figure 2.1).

- **Actuation based on movement of ions:** In this category, in addition to application of electric field, ions are required to make the actuation happen; therefore, the actuation occurs in a wet environment. Ionic electroactive polymers (also known as wet electroactive polymers) such as conducting polymers, and ionic polymer metal composites (IPMC) belong to this group. Recently it has been demonstrated that twisted carbon nanotubes can be actuated in electrolyte upon applying electric field [16].

- **Actuation based on thermal expansion:** A new type of electric field activated, electrolyte-free muscles called twisted yarn actuators has been recently introduced to the field [2]. The mechanism of operation is based on thermal expansion of a guest material within the conductive twisted structure. Materials with negative thermal expansion coefficient also can be engineered to actuate upon Joule heating.

$P \approx 0$ Gas inlet/outlet

$P > 0$
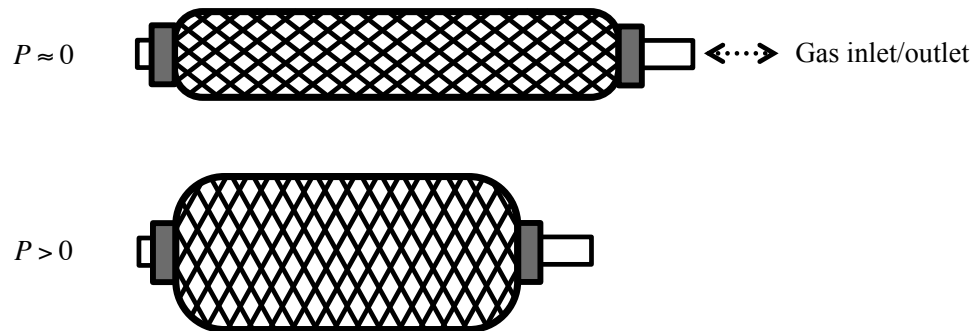
Figure 2.1 – McKibben artificial muscle. The pneumatic bladder is braded with stiff materials to allow high-pressure application.

In the human body most muscles work in pairs. One set of muscles, called 'agonist muscles', make the bone to move in a direction and the other set located on the opposite side of the bones or joints, called 'antagonist muscles', move the bone back to its original place. The same analogy may apply to the examples mentioned above. For some of the artificial muscles, relaxation of the muscle is only a function of time; therefore, reversing the applied voltage may not help to push back the actuator to its neutral position. As a result, utilizing the muscles in pairs can improve the functionality of the system. In contrast to electrically driven artificial muscles, in McKibben artificial muscles removing the pressurized air from the bladder fast, depending on the stiffness of the pneumatic bladder, can relax the muscle back to its natural state quickly.

In addition to electroactive polymers, piezoelectrics, magnetostrictives and shape memory alloys can generate linear and volumetric displacements when stimulated [17],[18], enabling them to be used as actuators. Though, none of these materials have demonstrated significant torsional actuation except when patterned in such a way as to convert linear motion into twist and untwist [19].

Carbon nanotube containing sheets and yarns have been shown to undergo dimensional changes when electrochemically charged in an electrolyte [20],[21] – like when an electrochemical double-layer capacitor is charged. A recent discovery has shown that the highly twisted carbon nanotube yarns, which have a built-in asymmetry (handedness), can be made to torsionally actuate when electrochemically swollen with ions [16] or when otherwise made to change in volume [2]. Wax exhibits a large volumetric expansion when heated (30% between 20°C and 210°C), [2] a property that has been previously used to achieve actuation, and is very effective in microactuators since the thermal time constants are small [22]. The impregnation of nanotube yarns with wax leads to exceptional actuation properties.

Niobium nanowire yarns provide a conductive matrix in excellent thermal contact with the inserted wax. The degree of yarn twist determines the extent wax volume change is converted to rotational actuation and linear motion. The stiff nanofibres, surrounded by expanding wax, are effectively inextensible. As will be explained in later chapters, three motions can result from an increase in yarn volume caused by expanding wax – a change in diameter, a change in length, and untwisting.

Artificial muscles can be used in various applications such as (bio)medical devices, toys, robotics, micro/nano electromechanical devices, and anywhere that muscle-type actuation is needed [23],[17].

The definitions of some important figures of merit in artificial muscles are listed below:

Stress (σ): is a measure of internal tractions or forces acting within a rigid body in a form of pressure or tension (Force/Area).

Strain (ε): is the change in the length of an object due to stress normalized to its original length ($\Delta L/L_o$).

Ultimate tensile stress: the maximum stress that a material can survive before it breaks.

Torsional Stiffness (κ): ratio of applied torsion moment to angle of twist (equivalent to spring constant but for twisted structures).

Young's Modulus (E): also known as tensile modulus or elastic modulus. The ratio of normal stress to linear strain [24].

Shear Stress (τ): Force exerting tangentially on a surface normalized by the surface area [25].

Shear Strain (γ): displacement of a surface relative to another normalized by the distance between them [26].

Shear Modulus: the ratio between shear stress and shear strain.

Work Density: Mechanical work done by the actuator normalized to its volume.

CHAPTER 3 – Materials and Methods[1]

In order to be able to analyze the mechanism of actuation we need to understand the mechanical and electrical properties of the yarn well. In this chapter, techniques used to prepare the sample and find the mechanical and electrical properties of the yarn are explained.

3.1 Sample preparation

A severe plastic deformation (SPD) process was employed to fabricate nano-scale niobium fibres. Nano-scale niobium fibres are extracted from copper-niobium composite wires that are drawn using a severe plastic deformation (SPD) process [27]. These composite wires were provided by National High Field Magnet Laboratory and supplied by Dr. Chad W. Sinclair. The SPD process used to create these wires involved accumulated drawing and bundling to produce a copper-niobium matrix [27]. The repetition of three hot-extrusion, cold drawing, and bundling cycles produce a sample with roughly 620,000 niobium nanowires in a cross-section with their axis being parallel to the axis of the matrix. The volume fractions of copper and niobium are 80% and 20%. Free-standing niobium nanowires were prepared by etching 4.0 mm diameter, 46 mm long sections (Figure 3.1) of copper-niobium wires in nitric acid solution (50% HNO_3 and 50% H_2O) at room temperature for seven days and then rising. Nitric acid was used because of its high selectivity (very slow etching of 0.025 mm/y for niobium). In order to achieve yarns of niobium rather than scattered individual nanowires, it is very important to secure both ends of the matrix and make sure the sample access the etching solution uniformly.
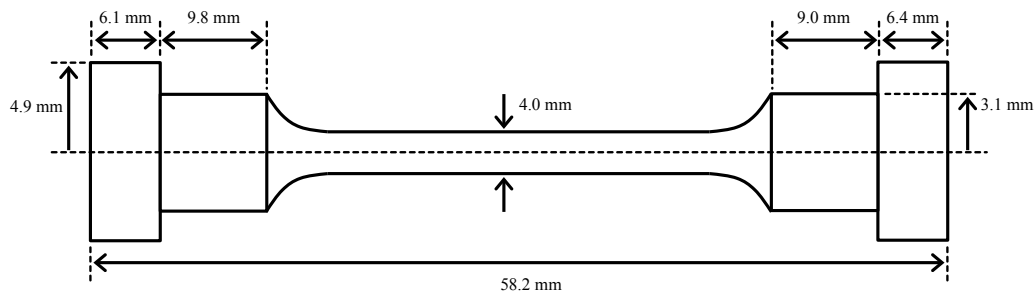
Figure 3.1 – Niobium – Copper matrix dimensions

The sample etching time was found to be roughly 170 hours. The etching started from the surface of the matrix and after about 10 min the surface was etched and inner parts were now exposed to the etchant. The solution was changed twice to ensure sufficient concentration of reagent. After the etching process completed, the sample was dipped into acetonitrile (CH_3CN) for three days (the solvent was changed six times) to ensure that the etchant is completely washed away. Elemental analysis was performed to determine the amount of copper remaining on the sample. The results showed that the copper was almost completely removed (appendix B, Figure A.6) as small nodules remain on the niobium fibres in some locations that are likely copper (Figure 3.2a) (based on the results from EDX-SEM measurements, appendix B). The resulting niobium wires are twisted to form a yarn (Figure 3.2b). In one of the samples, all of the copper in the matrix was etched to obtain pure niobium nanowires (for other purposes than making yarns). Figure 3.2c and Figure 3.2d show the clean niobium. More images are included in appendix C.
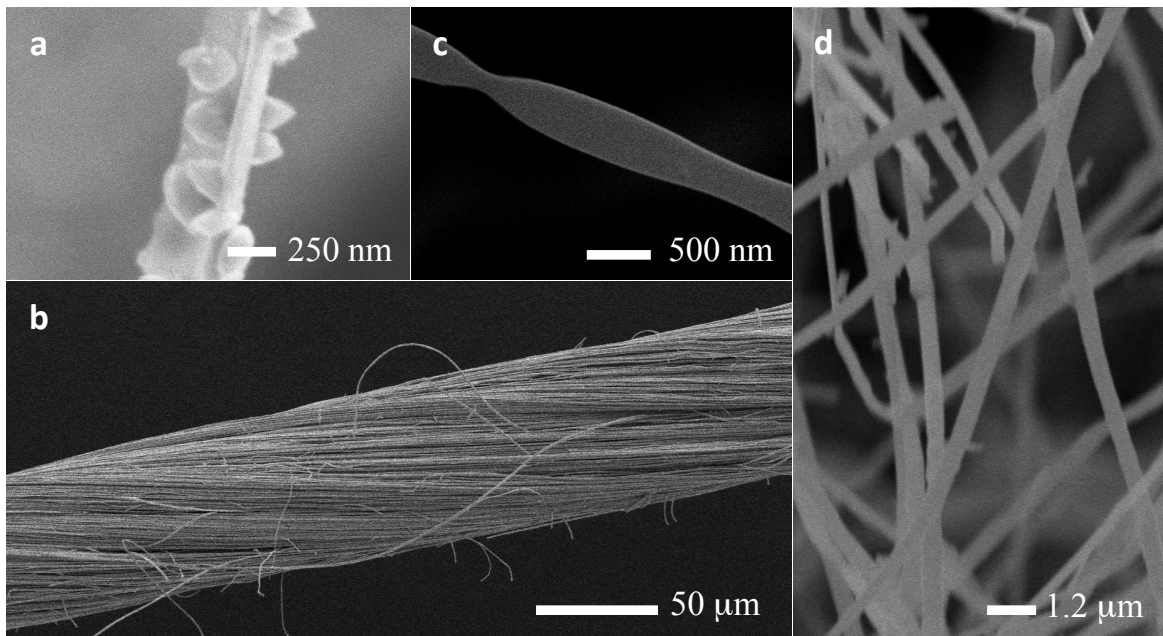
Figure 3.2 – SEM image of niobium fibres. a) close-up of fibres showing un-etched pyramids of copper on the nanowires, b) Niobium twist spun with twist angle α of 12°, c) one pure niobium nanowire which is like a twisted ribbon, d) mesh of pure niobium nanowires.

The niobium-copper wires are available in much longer lengths, since they are used as windings in ultra-high field magnets, so longer samples should be readily produced by using larger etching baths and longer starting lengths of wire.

Twist was inserted into the yarns by hand, and was between 1,200 and 5,300 turns per meter. The twist angle was in the range of 10° to 40° degrees. The technique used for twisting the yarns produces low twist angle yarns. In some samples twist was performed with a thin strand of hot-melt adhesive (Stanley Works GS15DT DualMelt™, referred to as a "polymer fibre") included in the twist (Figure 4.9). This addition made the yarn/strand combination less brittle.

Paraffin wax was added by hand, with a soldering iron used to melt in the wax. The wax employed is a low melting temperature wax (Glimma brand, paraffin/vegetable wax, IKEA).

3.2 Methods

To measure physical properties, linear and tensile actuation of niobium twisted yarns, the yarns were prepared (i.e. twisted and waxed) while the both ends were clamped to the measuring apparatus (Bose, Electroforce 3100). For the purpose of torsional actuation, a handmade apparatus was used.

3.2.1 Finding physical parameters

For elemental analysis we used a Philips XL30 Scanning Electron Microscope equipped with Bruker Quanta 200 energy-dispersion X-ray microanalysis system. The elemental analysis shows the ratio of copper to the niobium after the copper is etched. A uniaxial Bose Corporation Electroforce 3100 system was used as a muscle analyzer to measure the mechanical properties of the twisted yarn. Scanning electron microscope (Hitachi S-3000N SEM with light element EDX) was used to take images of the niobium nanowires and yarns.

Before stress-strain measurements were made on niobium yarns, the BOSE uniaxial device was tuned with a piece of twisted niobium yarn. Failing to tune the device properly can snap the yarns.

As shown in Figure 3.3, a load curve (input signal) is employed that consists of seven periods of a triangular wave input at a given stress amplitude followed by a five second hold, and then a repetition at the next amplitude, in eleven load steps. The output was logged and used to find the stress and strain.

The torsional stiffness (the spring constant in twist) was found by hanging a rod from the yarn in a torsional pendulum configuration, and recording the natural frequency of the twist via a video camera.

The diameters of the waxed/non-waxed parts of the yarns were measured by micrometer (Model Mitutoyo, Japan) with an uncertainty of ±5 to ±10 μm due to the pressure that the device clamp exert on the yarns during the measurement. Measured forces and displacements were normalized by initial measured dimensions of the samples loaded into the tensile testing apparatus, providing engineering stresses and strains.
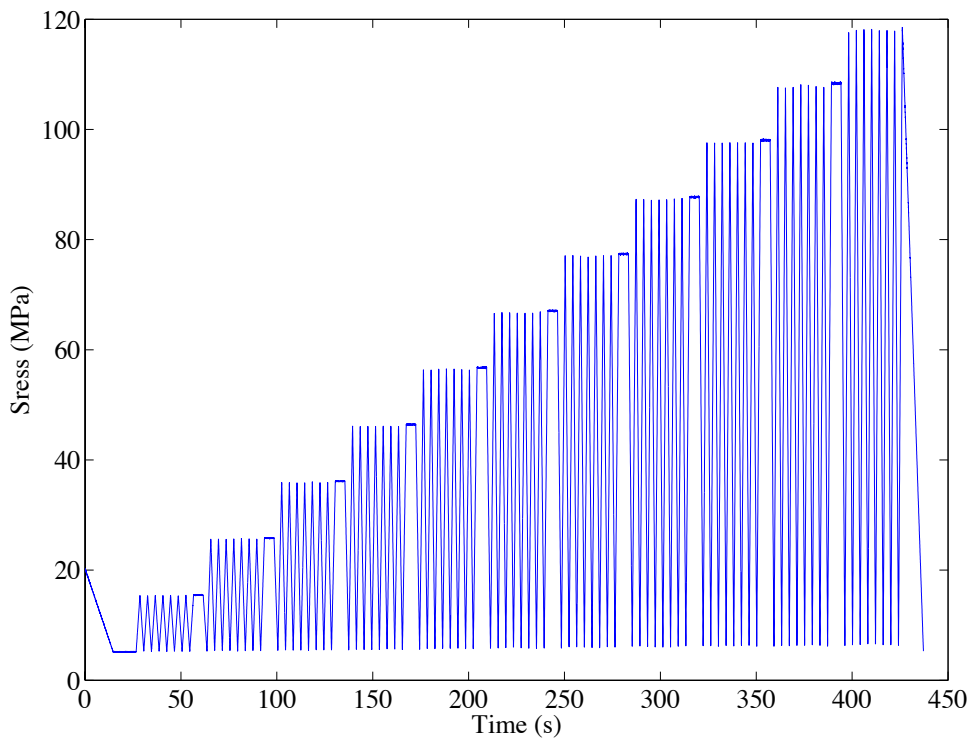
Figure 3.3 – The loading sequence used to determine stress-strain curves.

In order to study the thermal behaviour of the yarn during actuation, some of the tests were carried out under an infrared camera (High resolution thermographic camera, VarioCAM®). After running the experiment for a number of cycles, the same yarn was coated with Polyimide (HD-4010, HD Microsystems, DE, USA) to increase the emissivity of the niobium yarn in order to observe a more realistic value for the temperate at the surface of the yarn.

The melting point of the paraffin wax was measured with a thermometer (Kessler, ASTM 7C) to be 57°C.

Electrical conductivity of the yarns was found by applying voltage across the yarns and measuring the current and then using $V = RI$ to find the resistance.

The electrochemical capacitance of the yarns was found by cyclic voltammetry, using a Solartron SI 1287 Electrochemical Interface. Cyclic voltammetry involves a linear voltage sweep (from V_1 to V_2) between a working electrode (which is the niobium yarn in this experiment) and a reference electrode (Ag/AgCl electrode was used) and measuring the current in the counter electrode (Carbon paper). The capacitance can be found from the current and the voltage sweep rate from the following formula:

$$Q = CV \xrightarrow{\frac{d}{dt}} I = C\frac{dV}{dt} \Rightarrow C = I\left(\frac{dV}{dt}\right)^{-1}. \qquad (3.1)$$

In the formula above we have assumed the capacitance of the yarn does not change as a function time (i.e. $\frac{dC}{dt}V = 0$). In other words, the electrodes are held in place firmly and the yarn does not contract, expand, twist, or untwist. The mentioned parameters have some small effect on the capacitance; therefore, it is fair to assume the capacitance is not function of time.

The number of nanowires in a yarn cross-section can be found using the following techniques:

- **Mass-density:** by SEM imaging diameter of one nanowire can be found. Using the length of the yarn and density of the bulk niobium (8.57 g cm^{-3}), mass of each nanowire can be determined. Dividing the mass of yarn by the mass of each nanowire gives the number of nanowires.

- **Scanning Electron Microscopy:** Twisting the nanowires tightly into a yarn forms a closely packed structure. Measuring the diameter of the twisted yarn and the diameter of

each nanowire by SEM imaging, the number of nanowires can be determined using the following formula:

$$\frac{N \pi r^2_{nanowire}}{\pi R^2_{yarn}} \cong \frac{\pi}{6}\sqrt{3} \, , \tag{3.2}$$

where $\frac{\pi}{6}\sqrt{3} \approx 0.91$ is the density of hexagonal packing and N is the number of nanowires.

- **Capacitance:** By using a cyclic voltammetry technique, capacitance per area of one niobium 246 μm diameter wire was found $\left(\frac{C_{yarn}}{A_{yarn}}\right)$. Measuring the capacitance of the niobium nanowire yarn and using the following equation, effective surface area of the nanowire yarn can be found.

$$\frac{C_{wire}}{A_{wire}} = \frac{C_{yarn}}{A_{yarn}} \Rightarrow A_{yarn} = \frac{C_{yarn} A_{wire}}{C_{wire}} \, . \tag{3.3}$$

Assuming the diameter of one nanowire is D_{NW} and the length is L; the number of nanowires in the yarn can be found from:

$$N = \frac{A_{yarn}}{L \pi D_{NW}} \, . \tag{3.4}$$

Radius of nanowires can also be estimated by using the density equation, capacitance of the niobium yarn measured by the cyclic voltammetry technique (C), and capacitance per area (C_A) of the niobium macro wire by evaluating the following equation:

$$r = \frac{2 m C_A}{\rho C} \, , \tag{3.5}$$

where *m* is the mass of the yarn, and *r* is the density of the yarn.

3.2.2 Linear actuation

The linear actuation is performed by fully infiltrating the niobium twisted yarns with wax and applying square-shaped voltage pulses to the sample by opening and closing the circuit by hand. The yarns were clamped at both ends using the clamps of the muscle analyzer (Bose system) and then were twisted and infiltrated with paraffin wax in situ. In order to twist the yarns while the yarn was clamped at both ends, one small adaptor was made specifically for this purpose. The adaptor was placed between one of the clamps and the Bose system while the other clamps was attached to the load cell. The actuation was measured and recorded by the Bose uniaxial system (Bose Corporation Electroforce 3100).

3.2.3 Torsional actuation

The torsional actuation tests were performed by clamping the niobium yarns with two flat-head alligator clips, and rotating one of the clips around the axis of the yarn to insert twist. Figure 3.4 depicts the handmade apparatus used to insert twist.
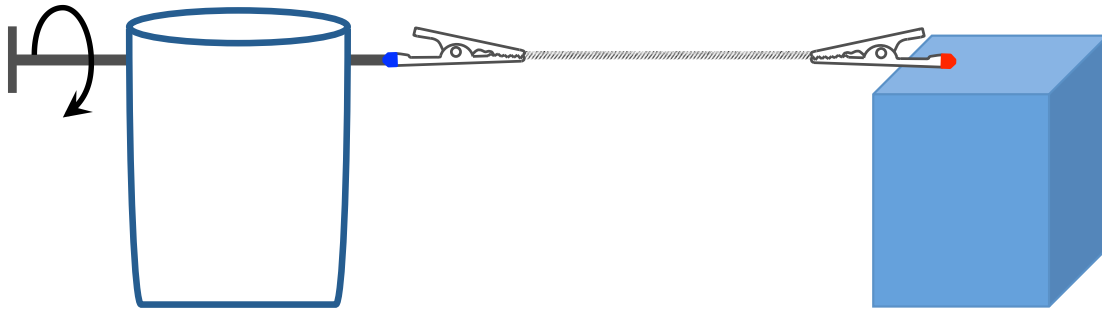
Figure 3.4 – The setup for twisting the yarns.

After twist insertion, half of the yarn was infiltrated with paraffin wax and a small paddle made of Copper tape was carefully attached to the middle of the yarn (Figure 3.5). Figure 3.6 clearly shows the border of the waxed and non-waxed portions of the yarn.
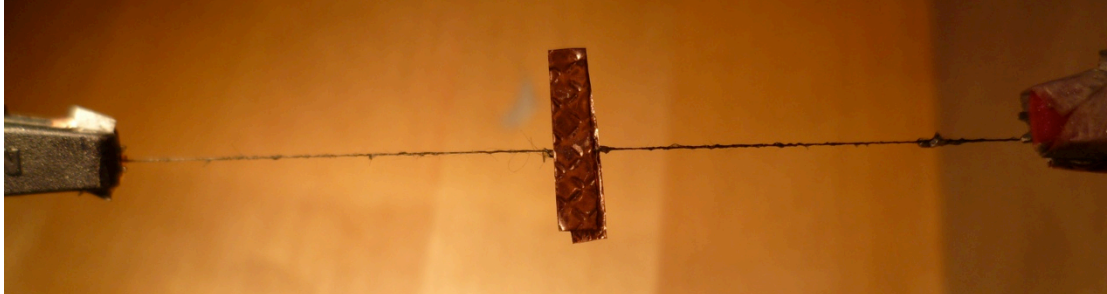
Figure 3.5 – The torsional actuation configuration, with the right half of the yarn infiltrated with wax and melting induced by current pulses.
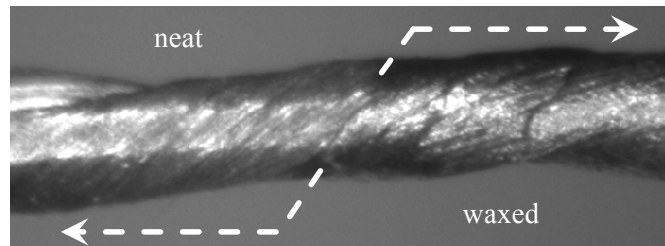
Figure 3.6 – Border of non-waxed and waxed part.

In a different configuration, two niobium yarns were twisted together with a thin strand of hot-meld adhesive (Stanley Works GS15DT DualMelt™) in the middle and in some samples around the niobium yarn. A function generator (Agilent, 33220A) was used to produce square shape pulses. To protect the function generator from possible shorting and current over loading, one N-channel power MOSFET (P16NF06) was used in a switch configuration (Figure 3.7) to allow for short pulses of larger current passing through the yarns. The actuation was captured by a high-speed video camera (Prosilica GE680 video camera, Allied Vision Technologies, Stadtroda, Germany).
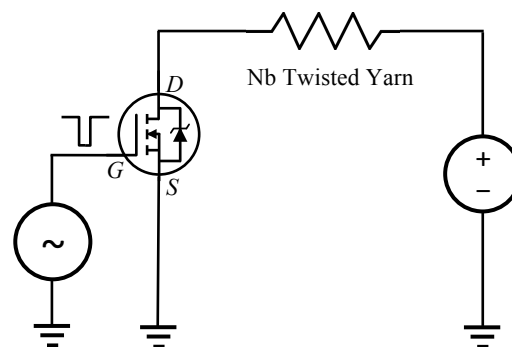
Figure 3.7 – Torsional actuator circuit model.

A multimeter (Fluke 110) was used to measure the resistance of the samples right before the actuation and also the applied voltage. The inserted twist angle (α) was determined by taking images of the sample and analyzing the images.

The techniques discussed in this chapter were implemented to produce the results presented in Chapter 4.

CHAPTER 4 – Results and Discussion[1]

This chapter presents the results obtained in different experiments with niobium yarns. Electrical and mechanical properties of niobium yarns as well as the actuation results are discussed here. Niobium yarns are compared to carbon multiwalled nanotube yarns due to the similarities between their properties.

4.1 Electrical properties of the niobium yarns

The conductivity of the niobium yarns was measured to be 3×10^6 S m^{-1} at room temperature, which is half that of bulk niobium and is large compared to the 3×10^4 S m^{-1} of carbon multiwalled nanotube yarns [15], [28]. The difference in conductivity suggests that for yarns of identical geometries about 10 times lower voltage can be used to generate the same heating power in niobium. The yarns burn in air at current densities above 3×10^6 A m^{-2} – which is similar to the current rating of insulated copper wires.

The electrochemical capacitance of the yarn provides an estimate of niobium diameter. The capacitance was measured to be 1.3×10^7 F m^{-3} at a scan rate of 25 mV s^{-1} in 0.2 M TBAPF$_6$ salt dissolved in acetonitrile; this value is similar to the capacitance per volume in carbon multiwalled nanotube yarns [1]. Based on the capacitance per volume and the capacitance per area measured in a macroscopic niobium wire of 0.25 F m^{-2}, and given the mass of the yarn and its length, the diameter of the individual niobium wires is estimated to be 90 nm. However, SEM imaging shows diameters of higher than 120 nm, which is within the 25% range. The number of individual nanowires per cross-sectional area of the yarn is $1.6 \pm 0.3 \times 10^{14}$ per m^2.

The density of the yarn for the sample in Figure 3.5 is 7.5 g cm^{-3}, suggesting that for the yarn there is ~13 % free space before wax insertion (based on the ratio of yarn density and that of bulk niobium, 8.57 g cm^{-3}).

---

[1] A version of this chapter is published. S. M. Mirvakili, A. Pazukha, W. Sikkema, C. W. Sinclair, G. M. Spinks, R. H. Baughman, and J. D. W. Madden, "Niobium Nanowire Yarns and their Application as Artificial Muscles," *Advanced Functional Materials*, 2013/adfm.201203808.

4.2 Mechanical properties

Stress-strain measurements were made on niobium yarn. As shown in Figure 3.3, the load curve (input signal) consists of seven periods of a triangular wave input at a given stress amplitude followed by a five second hold, and then a repetition at the next amplitude, in eleven load steps. The resulting stress-strain curves are in Figure 4.1 and Figure 4.2. Peak stresses for each set of the applied force triangles are indicated in the legend of Figure 4.2, and range from 15 MPa to 119 MPa.
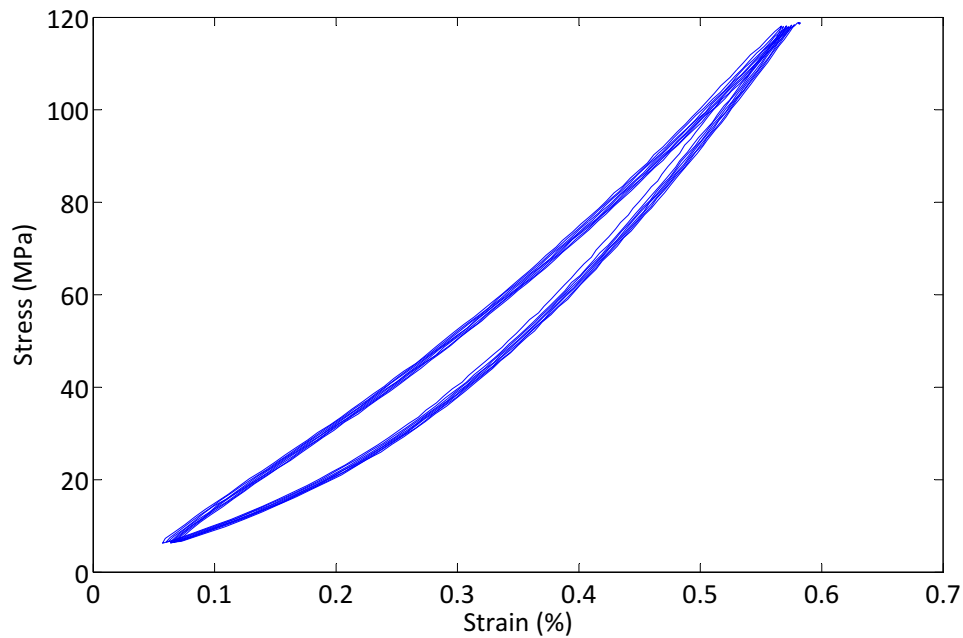
Figure 4.1 – Stress-strain curves obtained by repeated loading and unloading of a 110±15 μm diameter niobium yarn having an inserted twist of 516 turns per meter and a length of 31 mm. Maximum load of 118.7 MPa is achieved in the stress-strain curve.
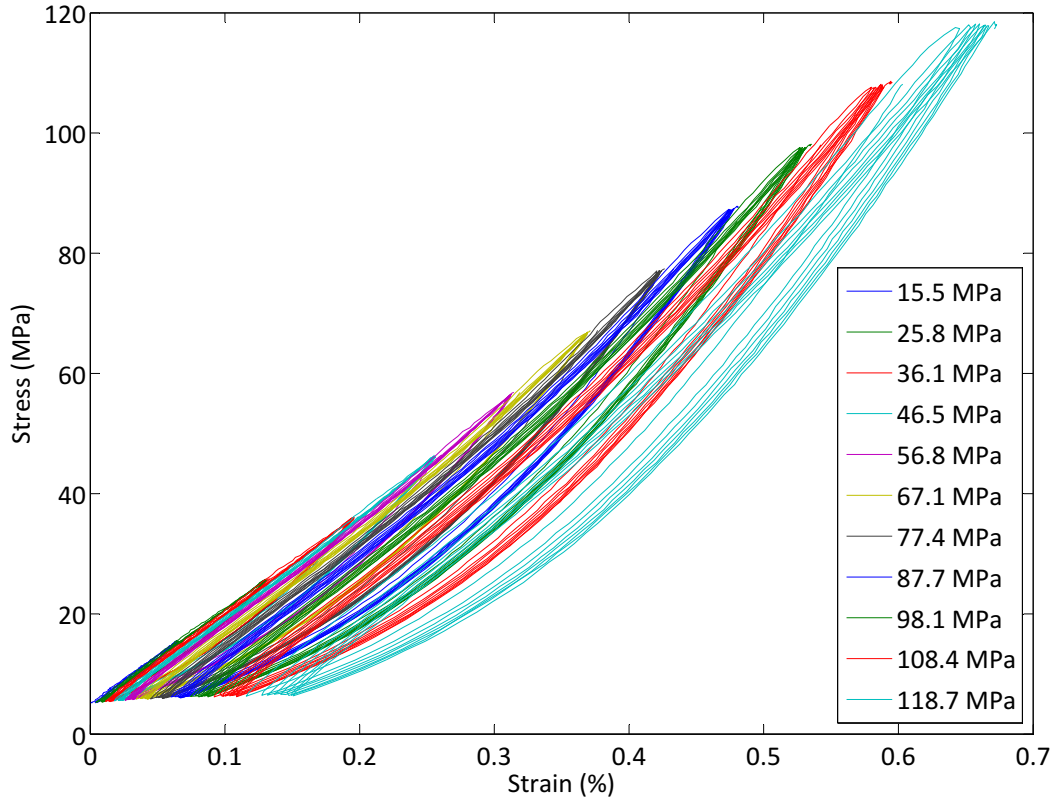
Figure 4.2 – Stress-strain curve obtained by successive tests on one niobium yarn sample having a 110±15 μm diameter, a twist of 516 turns per meter, and a length of 31 mm. The legend identifies curves by the maximum load achieved in a stress-strain curve for each cycle. There is a ~ 0.15% creep (stress relaxation) in the yarns. When the same yarn was subsequently used for other stress-strain measurements (Figure 4.1), creep was reduced to ~ 0.07% (almost half).

During the unloading cycles energy loss occurs, as indicated by the difference in area under the loading and unloading curves. Figure 4.3 shows the energy loss during the last ramp on each cycle. The energy loss and creep are smaller than that observed in wax-free twist-spun carbon multiwalled nanotube yarns [5] although the applied strain is ten times lower than for the carbon nanotubes yarn.
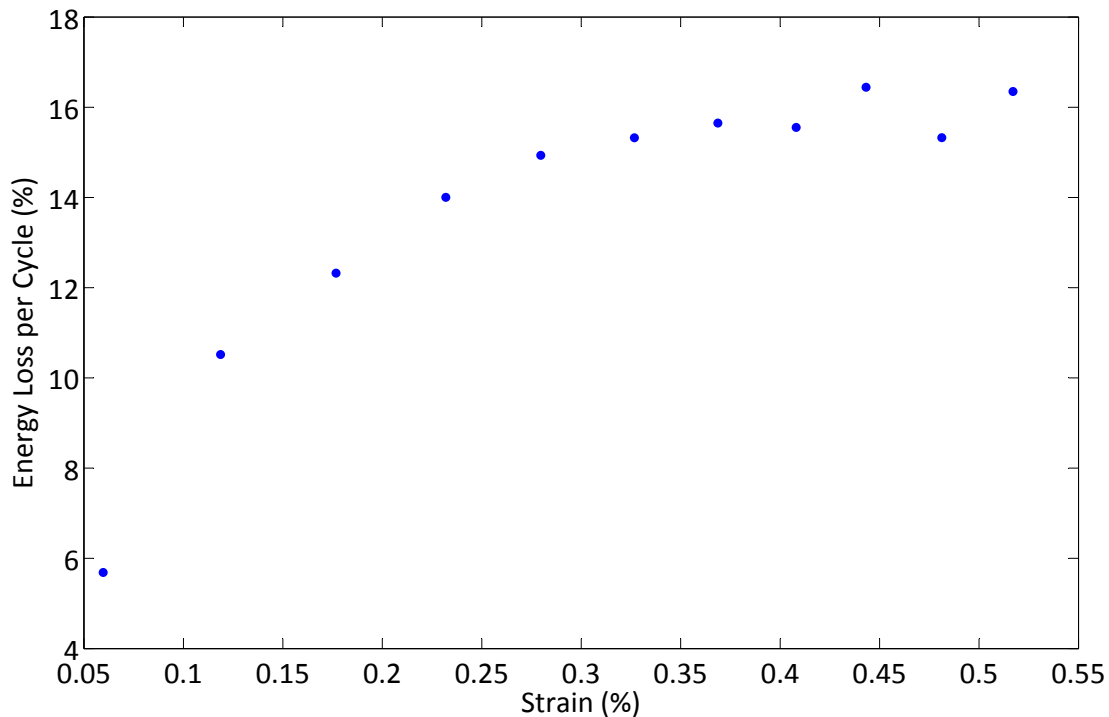
Figure 4.3 – Energy loss during loading cycles in Figure 4.2.

The neat niobium yarn tensile modulus of 19±5 GPa is found from the slopes up to 15 MPa stress (Figure 4.1 and Figure 4.2). This value is similar to the 15–20 GPa moduli seen in carbon multiwalled nanotube yarns [15]. The tensile modulus for fully wax-infiltrated yarns containing molten wax and solidified wax is found to be 7±2 GPa and 10±1 GPa, respectively.

The yarn showed a creep of ~ 0.07% over the period of the test, with larger creep being observed in the first run of this experiment (Figure 4.2). The tensile strength (Figure 4.4) reached 1.1±0.1 GPa in a 14 μm diameter sample, higher than the 460 MPa obtained in the carbon nanotube yarns employed in actuation [15] , but lower than the 2 GPa achieved for centimeter gauge length yarns spun from carbon nanotubes synthesized in the gas phase [29]. Thicker samples (20–50 μm) showed tensile strengths as low as 400 MPa, and that of the wax-containing yarn (80 μm diameter) is only ~110 MPa. The tensile strength appears to drop with increasing diameter, perhaps due to damage induced in the thicker yarns from the twisting. The niobium has a lower elongation at break than the carbon multiwalled nanotubes [3], [9], which may limit the achievable twist.
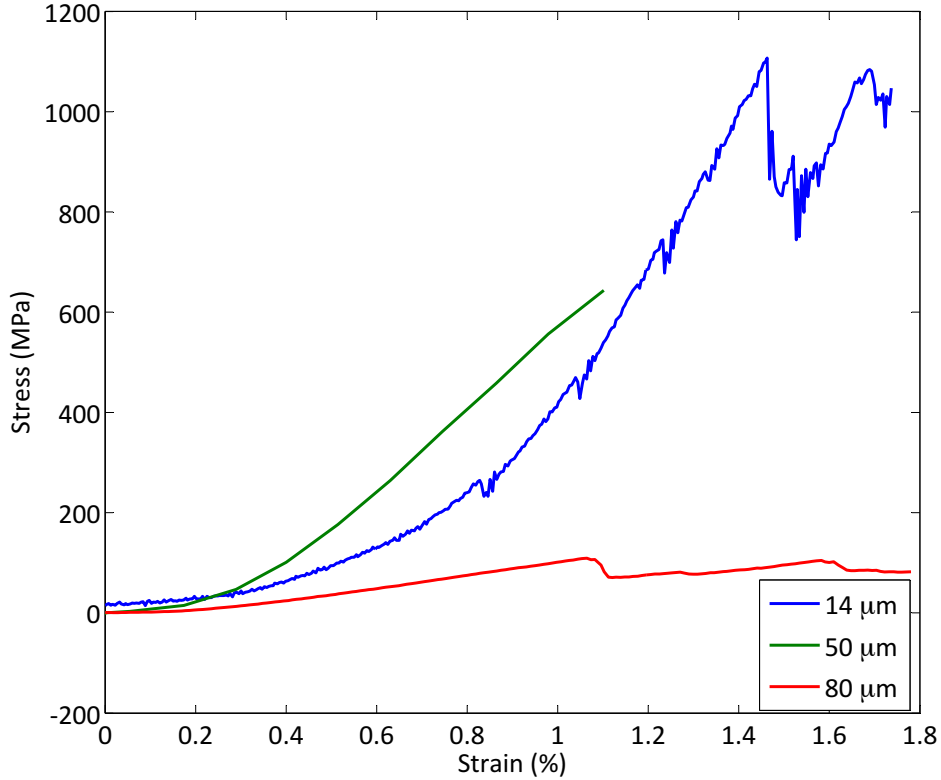
Figure 4.4 – Results of tensile tests of 14±1 μm, 50±1 μm, and 80±2 μm diameter yarns with identical inserted twists of 800 turns per meter. The 80 μm yarn was wax impregnated. The strain rates for these tests are 0.17% s^{-1}, 4% s^{-1}, and 0.33% s^{-1}, respectively.

The torsional stiffness is found to be 7.1×10^{-10} N·m rad^{-1} without wax, based on the torsional oscillation frequency of the yarn with a suspended paddle [25]. The shear modulus is estimated to be 17±6 GPa, which is similar to that estimated from torsional stiffness data in carbon nanotube yarns (17.7 to 21.6 GPa) [16]. Torsional stiffness in the waxed yarns is expected to be lower, probably by a factor of 1.5 to 2.5 seen in the tensile modulus. The torsional modulus of waxed yarn is not measured because the yarn would stay at its position and doesn't produce any torsional oscillation after inserting twist.

Torsional stiffness and shear modulus are estimated from the torsional oscillation period of a copper rod suspended at the bottom of a 3.3 cm long, ~180 μm diameter section of niobium nanowire yarn. The moment of inertia of the copper rod used in this experiment was $I \approx 5.24\times10^{-10}$ kg·m^2. Finding the natural frequency (by using a frame-by-frame analysis technique) and using $\kappa = I\,\omega_n^2$, the torsion spring constant is found to be $\approx 7.1\times10^{-10}$ N·m rad^{-1}. The shear modulus, G, is determined from the relationship $G = \frac{\kappa L}{J}$, where $J = \frac{\pi r^4}{2}$ is the torsion

constant, *G* is the shear modulus, and *L* is the length of the yarn. The shear modulus is found to be $G \approx 17 \pm 6$ GPa.

When the wax is added the yarn extends in length by about 0.5 %, as estimated from the stress relaxation observed in Figure 4.5, divided by the elastic modulus for the yarn with melted wax. The yarn diameter is found to increase by approximately ~100 % during the wax addition process. For a half-waxed yarn typical mass ratio (wax mass to the neat yarn mass) and volume ratio (wax volume to the neat yarn volume) are ~ 0.4 and ~1.1, respectively.
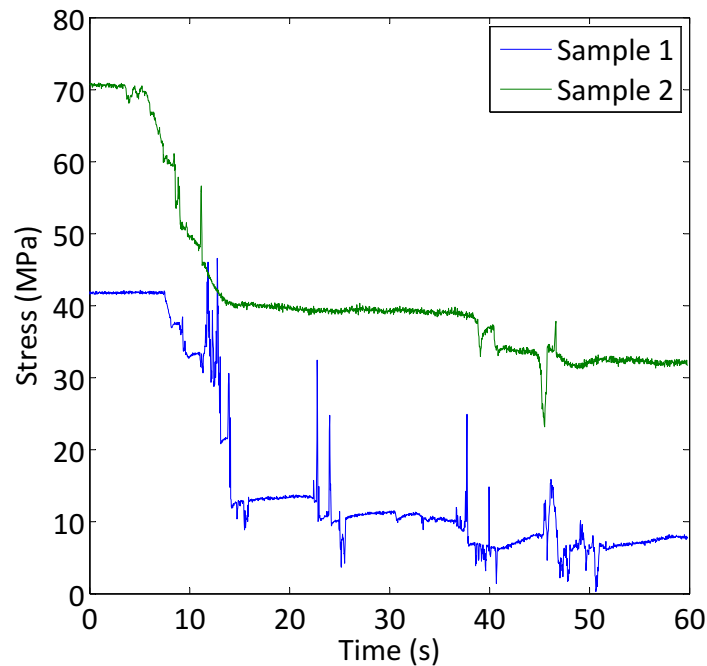
Figure 4.5 – Stress relaxation observed during wax impregnation. Twisted niobium yarns were clamped at both ends during the impregnation process. Sample 1 had 621 turns per meter with resistance of 34 Ω (10.3 Ω cm⁻¹) and diameter of 89 μm and Sample 2 had 588 turns per meter with resistance of 57 Ω (16.8 Ω cm⁻¹) and diameter of 67 μm. Sample 1 and 2 relax down by ~ 34 MPa and ~ 39 MPa during the impregnation process, respectively.

4.3 Linear actuation

Linear contraction of the yarn is observed upon melting (and swelling) of the wax, as expected at twist angles below 57 degrees [16]. Upon applying 1.03 V cm⁻¹ to a 3.4 cm niobium yarn with resistance of 22.4 Ω, 7 MPa increase in stress is produced when the yarn is Joule heated (3.6 kW cm⁻³) under isometric (constant length) conditions (Figure 4.6).
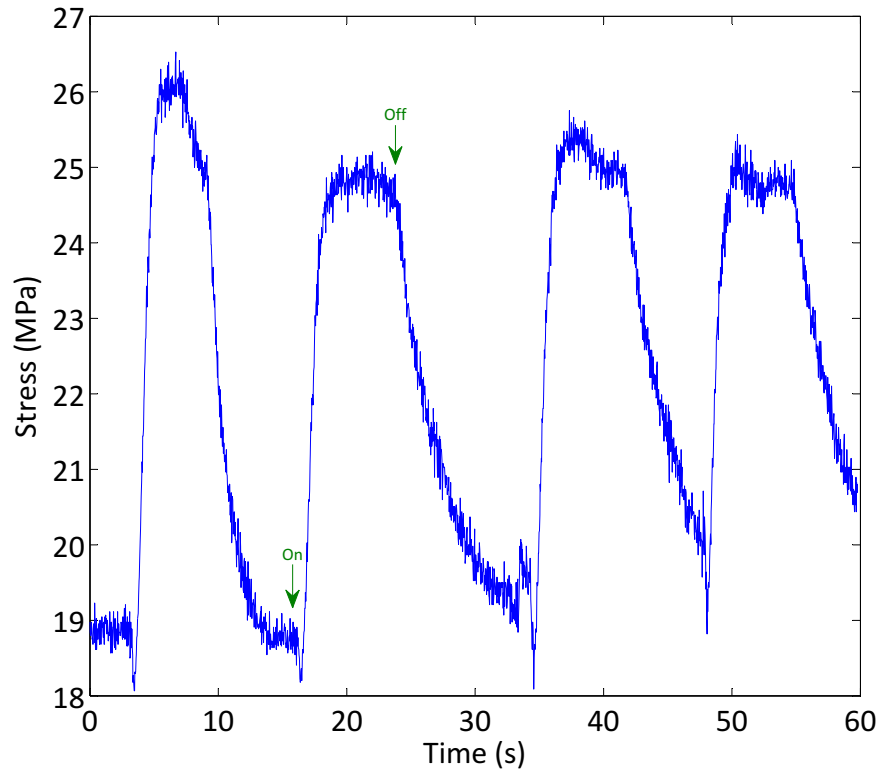
Figure 4.6 – Change in yarn stress during melting and solidification of wax-impregnated yarn when length is held constant. An applied voltage (1.03 V cm^{-1}) is switched "On" and "Off" at the times indicated by arrows. The yarn is 74±5 μm in diameter and has 603 turns m^{-1} of inserted twist, which produced a twist angle of 8°. The 3.4 cm yarn length between clamps had 22.4 Ω in resistance and the input thermal power per cycle (normalized to yarn volume) was 3.6 kW cm^{-3}, most of which was used to maintain the yarn in the actuated state. Over 27 cycles of linear actuation, the average change in stress was 7 MPa.

The change in stress observed was consistent over the 27 cycles of the experiment. In addition, an effective strain of ~ 0.24 % at an input electrical power of 3 kW cm^{-3} was observed over 55 cycles for a yarn kept at constant load of 20 MPa (further information in appendix B). The theory (equation 4.5) predicts an effective of stain of ~ 0.29 % which is very close to the practical value. The strain is two times larger than that observed in a non-coiled wax infiltrated carbon multiwalled nanotube yarn [2]. Larger linear expansion should be achievable by increasing twist angle [16], and ultimately by generating coiling, as is observed in carbon multiwalled nanotube yarns [2]. Increasing twist angle has not proven practical thus far in

niobium yarns, and may be limited by failure of the outer niobium fibres as a result of the tensile strain induced during twisting.
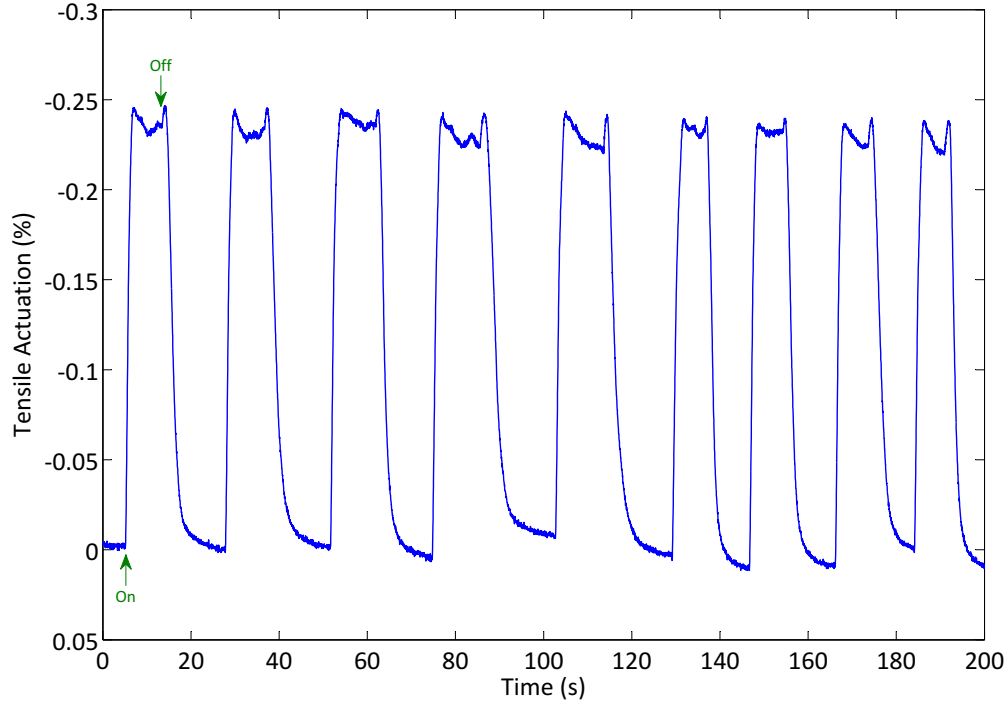
Figure 4.7 – Tensile actuation of the wax-impregnated yarn at constant load of 20 MPa. The times when the applied voltage (1.11 V cm^{-1}) is switched "On" and "Off" are indicated. The yarn is 78±5 μm in diameter and has 796 turns/m of inserted twist, which produced a twist angle of 11°. The 2.7 cm yarn length between clamps had 22.9 Ω in resistance and the input thermal power per cycle (normalized to yarn volume) was 3 kW cm^{-3}. Over 55 cycles of linear actuation, the average change in strain was 0.24%. Due to the thermal expansion of the yarn itself there is an initial rise in strain on switching off the current, followed by a drop due to wax change in volume. The neat yarn thermal expansion is apparent in the increase in stress seen when the current is turned off, shown in Figure 4.8.
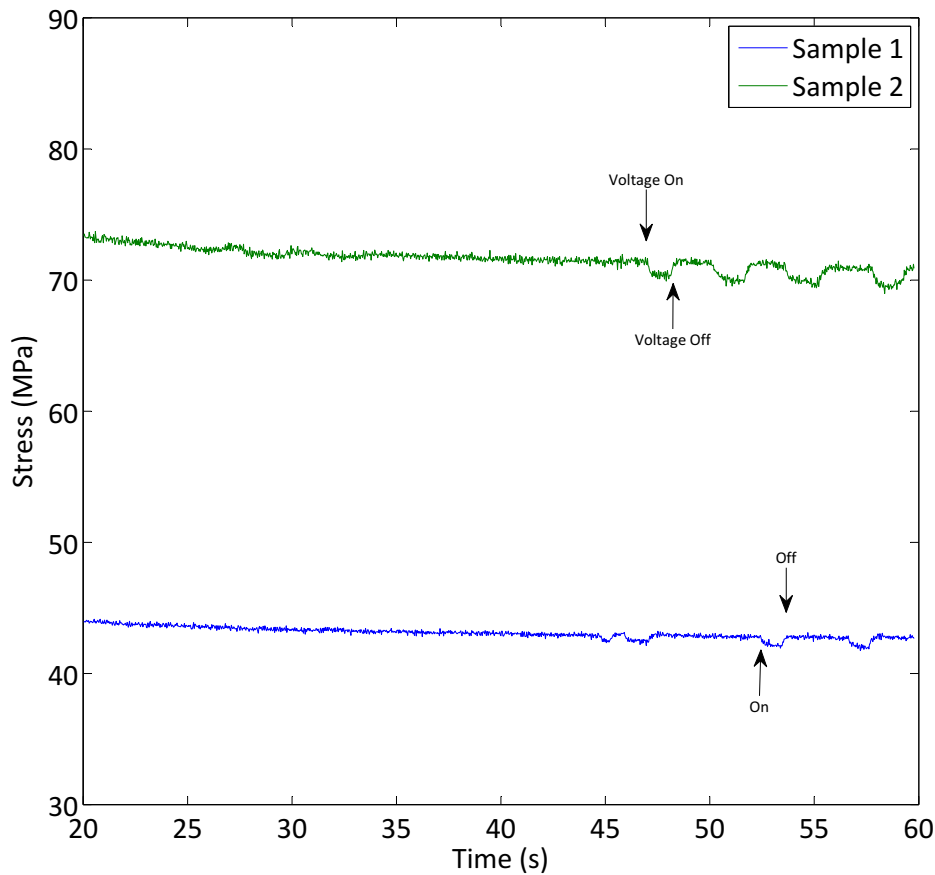
Figure 4.8 – Actuation of a wax-free niobium yarn, showing thermal expansion when heated. Sample 1 had a diameter of 89 μm, an inserted twist of 621 turns/m and a resistance of 34 Ω (10.3 Ω cm⁻¹) and was actuated with square shape pulses of 585 mV cm⁻¹. Sample 2 had a diameter of 67 μm, a inserted twist of 588 turns m⁻¹ and a resistance of 57 Ω (16.8 Ω cm⁻¹), and was actuated with a square shape pulses of 500 mV cm⁻¹.

In Figures 4.6 and 4.7 there are small spikes at the turn on/turn off events. At the moment the voltage is applied to the yarn, the yarn starts heating. A small portion of the responses in Figure 4.6, and Figure 4.7 is due to thermal expansion of the niobium yarn itself (Figure 4.8), where the ~1 MPa change in stress (~ 0.005% strain) accounts for the initial drop in stress seen in the waxed yarns when current is applied. In Figure 4.7, it accounts for ~ 0.015% strain. This drop in stress is primarily due to the non-waxed portion of the yarn, where higher temperatures are reached, as seen in the thermal camera generated videos.

4.4 Torsional actuation

Active rotational actuation was obtained by infiltrating wax into the yarn, which was then alternately electrically melted and re-solidified to induce untwist and then re-twist. As suggested in work on carbon nanotube yarns [16], half of the yarn's length is infiltrated with wax, with the other half of the yarn providing a restoring force to assist recovery of the twist (Figure 3.5). Melting is produced by applying 0.32 V cm^{-1} (890 W cm^{-3}) to 12 V cm^{-1} (30 kW cm^{-3}) to the sample shown in Figure 4.9a via square pulses through the yarn, thereby providing a range of input power to volume from 300 W cm^{-3} to 30 kW cm^{-3}.
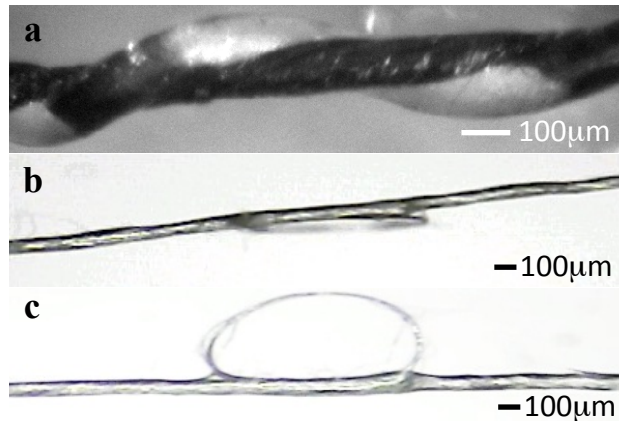
Figure 4.9 – a) In this sample a polymer fibre with diameter of 116 μm is wrapped around a twisted niobium yarn with diameter of 98 μm, inserted twist of 1,300 turns m^{-1}, and resistance of 57 Ω cm^{-1}. The yarn could survive high voltages of up to 40 V (12.1 V cm^{-1}). b) Top view and c) front view of the loop on the twisted yarns with one strand polymer fibre.

Figure 4.10 presents an example of the temperature profile obtained for a case where a pulse of 1.36 V cm^{-1} is applied (300 W cm^{-3}) for ~8 s. The image indicates that there are lower temperature sections of the yarn (middle and left portions). These correspond to wax-filled regions. Presumably the higher heat capacity and large latent heat of melting of these wax-infiltrated regions leads them to be cooler. The waxed regions also have longer thermal time constants for heating and cooling, as observed in time sequences shown.
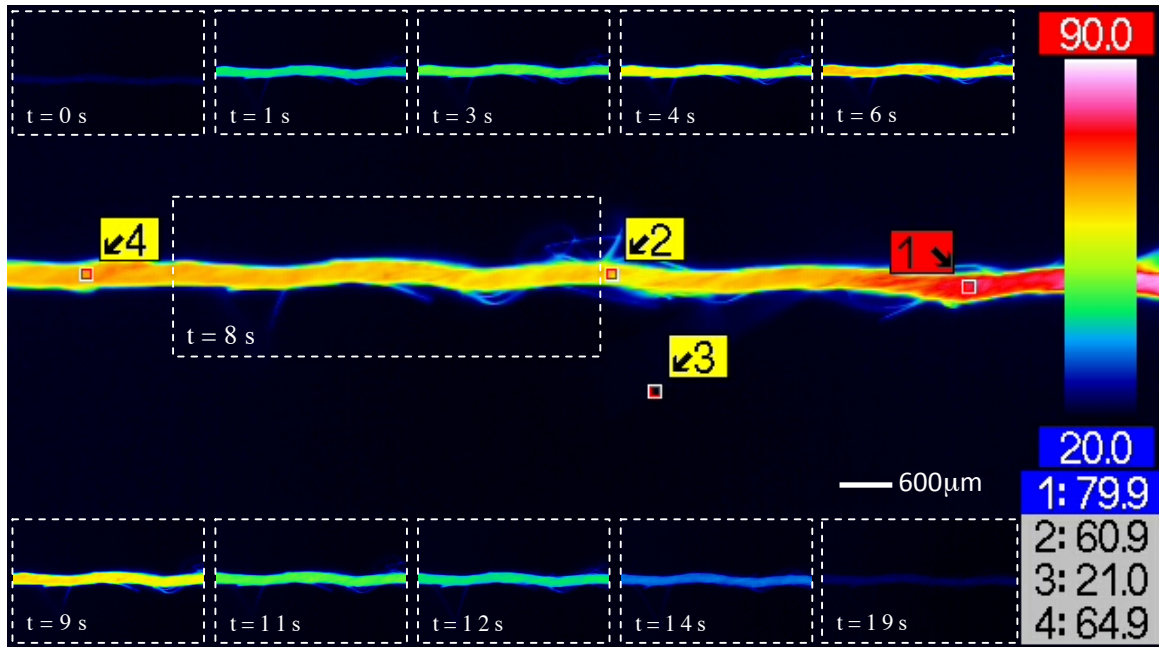
Figure 4.10 – Thermal profile of a half-wax-infiltrated yarn three seconds after the application of a square wave voltage pulse of 1.36 V cm^{-1}. The red region is without wax. Arrows and the legend correspond to the approximate temperatures reached. The yarn diameter without wax is 310 μm, the total yarn length between clamps was 22 mm, and the input power per volume was 300 W cm^{-3}. The emissivity of the niobium is < 1 so the temperature scale may underestimate the true temperature at the surface of the yarn.

Rotation as a function of time in response to a 100 ms long pulse is shown in Figure 4.11, as determined by frame-by-frame video analysis at 200 frames per second. There is an initial rapid unwinding (blue line) in response to a voltage spike (dashed line), followed by a damped oscillation and a gradual re-twisting. The cooling time constant of several hundred milliseconds determines the rate of recovery of the twist. In this experiment the rotation rate reaches 650 RPM, which is similar to the 592 RPM achieved in electrochemically driven carbon nanotube yarns, but slower than the 11,500 RPM average torsional rotation rate demonstrated in wax infiltrated carbon nanotube yarns. The resonant response, as indicated by the damped oscillation following the 100 ms excitation (Figure 4.11), demonstrates that paddle inertia is playing an important role in limiting the rate.
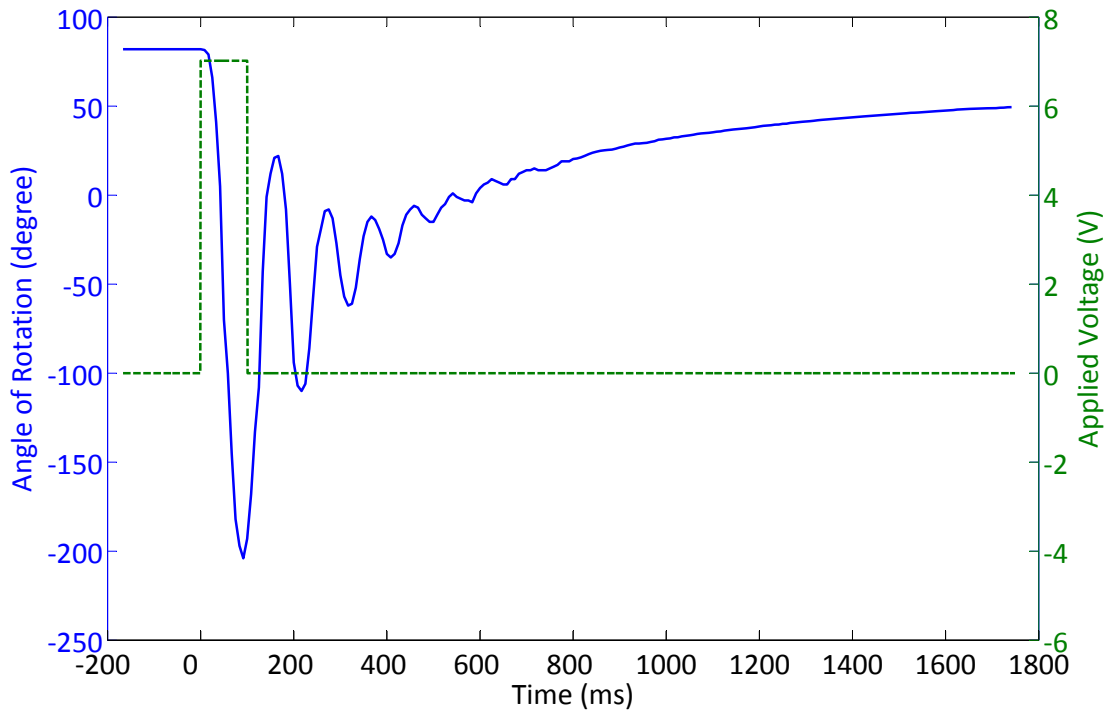
Figure 4.11 – Angle of rotation versus time upon pulse voltage actuation of the niobium yarn and paddle shown in Figure 3.5. The resistance is 35 Ω and melting is produced by a 100 ms square pulse with amplitude of 7.02 V, represented by the dashed line. The power per volume produced by this pulse is 11 kW cm^{-3}.

The initial acceleration of the paddle (Figure 4.11) is found to be 2,500 rad s^{-2} (150,000 deg s^{-2}). Given the initial angular acceleration, and the paddle moment of inertia ($I = m\frac{L^2+W^2}{12}$, with m = 22.49 mg and I = 3.34×10^{-10} kg·m^2), the torque produced is 0.8 mN·m. The mass of the active portion of the yarn and the wax is 960 µg, and the torque to mass ratio is 0.9 N·m kg^{-1}. The torque to mass is about 1/10th that of wax-infiltrated carbon nanotube yarns [2], and the torque to volume is about 1/3rd as large. The heating power per volume is higher in the niobium case, suggesting that the rate of heating is not the cause of the lower torque per volume. Given the resonant response, the paddle inertia is almost certainly limiting rate. The lower twist angle (21°) compared to those of the nanotube yarns (up to 43°) is an important factor reducing the torque and speed generated, as discussed below. The torque to mass ratio is nevertheless substantial – at about 1/4 that produced by commercial direct drive motors [18]. The power to mass is 35 W kg^{-1} ($\frac{1}{2}\frac{I\omega^2}{\Delta t}$), compared to 61 W kg^{-1} obtained in electrochemically driven carbon

nanotube yarn actuators [16], with the power to volume in the niobium yarn being higher than in these electrochemically driven carbon nanotube yarns.

Fast torsional actuation was achieved by using a loop of yarn to observe twist instead of a paddle (henceforth a "paddle-free yarn") in a half-waxed yarn. In this low inertia paddle-free yarn, that is once again half waxed, the peak rotation rate reaches at least 1,800 RPM. This rate is determined by the observed 360-degree rotation in less than one video frame ($1/30^{th}$ of a second) upon application of a 4.8 V pulse (3 kW cm^{-3}). The theory (equation 4.3) predicts 1.5 turns, which is very close to the experimental value. Untwist is slower, taking about 1 s, due to the thermal time constant of the yarn. This thermal time constant should be dramatically reduced in thinner yarns, as found for carbon multi-walled nanotubes, where 11.5 μm diameter yarns show a large recoverable response at 20 Hz, while 150 μm yarns have a time constant of more than a second. The niobium yarns were twisted and manipulated by hand, making it a challenge to achieve the very thin yarns machine spun from carbon nanotubes.

To improve the mechanical stability and actuation performance of very thin yarns the niobium yarn is combined with a polymer fibre. In the structure of this fast acting sample, two niobium yarns were twisted together with a thin polymer fibre (Figure 4.9b, Figure 4.9c), which resulted in some coiling and an increase in heat capacity. The yarn employed is 3 cm long and 60 μm in diameter, with an inserted twist of 2,300 turns m^{-1}. Increasing pulse voltage amplitude leads to faster rotation (up to 7,200 RPM), but also to burning (Video 2, Supplement of Materials [30]). Observations in other yarns indicate that burning of the yarn and the resulting failure begins near the center of the yarn where the wax-free and waxed portions of the yarn meet. The non-waxed portion of the yarn reaches higher temperatures than the waxed portion, presumably due to its lower heat capacity, leading to the ignition of the neighbouring waxed regions. Adding the polymer fibre strand increases the heat capacity, which results in lower temperatures on the neat side of the yarn, and may enable higher wax temperatures before failure in the yarn is observed.

Inertia no longer appeared to be limiting the rate of twist in these paddle-free yarns. This was evident in the lack of oscillation seen in the responses of these yarns. The speed of response and torque are likely instead to be set by the heating rate. The use of shorter pulses for which

thermal energy is carefully controlled may lead to even faster rotation while avoiding burning. Increasing length and twist angle, as well as reducing thickness of the yarn should also lead to faster rotations. The twist achieved in the niobium is not as large as that in carbon nanotube yarns, perhaps because carbon nanotubes exhibit higher elongation at break and greater tensile strength than the niobium nanofilaments. The result of lower twist is less rotation per actuator length, and for the same heating rate, lower rotation speed. In addition, the large niobium diameter, compared to CNT diameter, can play a role in reducing the allowable twist on the niobium yarn.

The higher electrical conductivity of the niobium yarns enables lower voltage operation than in carbon MWNT yarns for the same heating rate. Lower voltage operation is beneficial in portable battery operated applications (e.g. toys, valves and implanted medical devices). The 310 μm diameter yarn used to generate the data in Figure 4.10 is activated using 1.36 V cm^{-1}, whereas a 150 μm carbon nanotube yarn [2] activated over a similar time frame employs 15 V cm^{-1}. A centimeter length of the niobium yarn thus requires only a single alkaline cell to activate, whereas the same length of nanotube yarn needs ten.

In addition to the torsional actuation, an isotonic (constant force) tensile (linear) actuation of 0.24 % was observed, as shown in Figure 4.7. This strain is larger than that achieved for a non-coiled carbon multiwalled nanotube yarn, but much smaller than for the coiled nanotube yarn [2].

The presence of torsional actuation in both the carbon nanotube and the niobium nanowire yarns confirms that the actuation is not specific to carbon. Indeed, torsional actuation might be expected in any helically wound structure in which a volume change is induced as long as the yarn guest can remain confined in the yarn. The use of nanofibre yarns provides surface energies that result in wax confinement when the interfacial energy between nanofibre and air is much less energetically favourable than between guest and nanofibre.

4.5 Actuation mechanism

When wax is melted within the niobium yarn, changes in length, diameter and twist result. The approximate magnitudes and directions of these responses can be predicted by modeling the fibres that make up the yarn as inextensible, and considering the effect on the outermost fibres,

for the case when twist is prevented [1], and the general case of elongation, twist and radial dilation [16]. The niobium yarns have a twist angle (α in Figure 3.2b), which is the angle the outer fibres make with the yarn axis, given by [16] (derivation in the appendix A):

$$\alpha = \tan^{-1}(2\pi r T) \,,$$

(4.1)

where r is the distance from yarn center and T is the inserted twist in turns per yarn length [16]. Volume expansion at constant length is associated with yarn untwist which in turn enables an increase in yarn diameter, as depicted in Figure 4.12. If the yarn is not allowed to change twist (for example if both ends are clamped), then yarn volume increase is predicted to be associated with a contraction in length and an increase in diameter for twist angles that are sufficiently small (Figure A.1). It was shown that for inextensible outer fibres the relationship between the final number of turns, n, the initial number of turns, n_o, the length of the helically wound fibres on the surface of the yarn, L_s (these are assumed to extend the entire length of the yarn, L_o), and the ratio of final length to initial length, λ is:

$$\frac{n}{n_o} = \sqrt{\frac{V_o}{V} \cdot \frac{\lambda L_o L_s^2 - \lambda^3 L_o^3}{L_o L_s^2 - L_o^3}} \,,$$

(4.2)

where V_o is the initial volume, and V is the final volume [16]. In the situation where length remains constant ($\lambda = 1$), a drive to increase yarn volume (by heating the wax) is expected to produce a reduction in the number of turns, Δn, as given by:

$$\frac{\Delta n}{n_o} = \left(\frac{V_o}{V}\right)^{1/2} - 1 \,.$$

(4.3)

Figure 4.12 depicts the effects of a volume increase with the yarn held at constant length. The length of the helically wound fibres (red, blue and green) stay constant as the yarn increases

in volume. Untwisting must occur in order to enable the diameter increase and volume change, while keeping the fibre and yarn lengths constant.
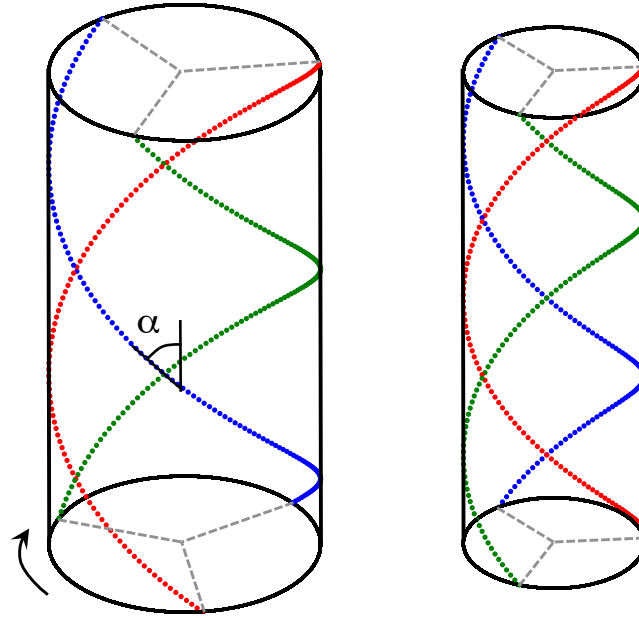
Figure 4.12 – The wax expands and that leads to volume expansion of the twisted the yarns. The blue, red, and green dot lines demonstrate three strands of niobium nanowires twisted together. The length of the yarn is kept constant and the twist at the top is also kept constant. As the radius increases by dr the structure expands by untwisting the yarn by $d\varphi$ (the left diagram) and thus generating rotation (torsional actuation). The twist angle (α) is the angle between the yarn length axis and the fibre direction.

Equation 4.3 suggests that the change in twist, Δn, is not only a function of volume, but also of initial twist per unit length, n_o. This twist can be expressed in terms of the initial twist angle, α (Equation 1, Figure 3.2b) and the initial yarn radius, r, such that the change in number of turns is:

$$\Delta n = \left(\left(\frac{V_o}{V}\right)^{1/2} - 1\right)\frac{L\tan(\alpha)}{2\pi r} \ . \tag{4.4}$$

The equation provides an estimate of the number of turns expected if length is held constant (isometric conditions). Equation 4.4 predicts that larger initial twist angle and longer length, as well as smaller yarn diameter, will all lead to a greater change in twist. In cases where

heating rate limits actuation speed, faster rotation should be achieved by using longer yarns, thinner yarns and/or yarns that have more turns per meter (and hence a higher α).

Carbon multiwalled nanotube yarns have achieved higher rotation speeds. The fast niobium yarns presented in the main text however have a lower twist angle (20° for niobium vs. 35° for the carbon nanotube case, leading to a factor of two difference) and more importantly the smaller ratio of yarn length to diameter (factor of five) [2]. Increasing the length of the niobium yarns, as well as the twist, could then increase the number of turns produced, and also the speed of response, leading to an increase of a factor of ten or more in rotation rate.

In order to estimate strain when rotation is prevented, equation 4.2 can be adapted for the case where $n = n_o$. Given that the extension ratio, λ is L/L_o, which is equal to $1+\varepsilon$, where ε is strain, then assuming strain is small ($\lambda^3 \cong 1 + 3\varepsilon$) it can be related to change in volume and yarn geometry by (full derivation in appendix A):

$$\varepsilon = \frac{\Delta V}{V_o} \frac{\tan^2(\alpha_o)}{\tan^2(\alpha_o) - 2} \ .$$

(4.5)

As in a McKibben actuator, strain is expected to be maximum at α = 54.7°. For the case of yarns, the outer yarn angle will be larger than the inner angles, so a larger angle will be needed in order to reach the maximum. Recent work has shown that strain can be further amplified by using coiled yarns [2]. Coiling is an effect that occurs in highly twisted yarns, and is common seen in rubber bands (e.g. in twisting the band used to power a toy plane). In coiling the yarn itself forms has a helical twist (and not just the fibres that make the yarn).

CHAPTER 5 – Conclusion and Recommendations[1]

In this thesis, it is demonstrated that metal nanowires such niobium can be engineered to form strong yarns similar to carbon nanotube yarns while maintaining their electrical properties. This can be a new sister to the widely studied carbon nanotube yarns. The great mechanical and electrical properties that the niobium yarns offer enable them to be utilized in as artificial muscles and potentially other applications.

The artificial muscle was made by twisting and then impregnating the niobium yarns with paraffin wax. By applying voltage across the niobium yarn joule heating occurs which leads to melting the wax. Due to the large thermal expansion of the wax, according to the helical model, the yarn untwists and then retwists when the wax cools down. This idea can be applied to many other applications. Table 1 compares some properties of niobium yarns with carbon multiwalled nanotube yarns.

Table 1 – Comparison between properties of niobium nanowire twisted yarns and twist-spun carbon multiwalled nanotube yarns.

	Niobium Nanowire Twisted Yarn	Twist-spun Carbon Multiwalled Nanotube Yarns
Conductivity	$3 \cdot 10^6$ S m^{-1}	$3 \cdot 10^4$ S m^{-1} [15], [28]
Ultimate Tensile Strength	1.1 GPa	460 MPa [15]
Young's Modulus	19±5 GPa	15 to 20 GPa [15]
Shear Modulus	17±6 GPa	18 to 22 GPa [16]
Tensile Actuation	0.24% (@20 MPa)	0.12% (non-coiled @4.8 MPa) [2]
Torsional Actuation Speed	7,200 RPM	11,500 RPM [2]
Torque to Mass	0.9 N·m kg^{-1}	8.4 N·m kg^{-1} [2]

In conclusion, this work demonstrates that the mechanism of torsional actuation works in materials other than carbon multiwalled nanotubes. As has been shown for carbon nanotubes, mechanical properties of niobium yarns are enhanced by a great factor when they are twisted.

---

[1] A version of this chapter is published. S. M. Mirvakili, A. Pazukha, W. Sikkema, C. W. Sinclair, G. M. Spinks, R. H. Baughman, and J. D. W. Madden, "Niobium Nanowire Yarns and their Application as Artificial Muscles," *Advanced Functional Materials*, 2013/adfm.201203808.

The high electrical conductivity that is observed for niobium yarns in this works, opens a door to lot of applications in different fields.

BIBLIOGRAPHY

[1] T. Mirfakhrai, "Carbon nanotube yarn actuators," 2009.

[2] M. D. Lima, N. Li, M. J. de Andrade, S. Fang, J. Oh, G. M. Spinks, M. E. Kozlov, C. S. Haines, D. Suh, J. Foroughi, S. J. Kim, Y. Chen, T. Ware, M. K. Shin, L. D. Machado, A. F. Fonseca, J. D. W. Madden, W. E. Voit, D. S. Galvão, and R. H. Baughman, "Electrically, Chemically, and Photonically Powered Torsional and Tensile Actuation of Hybrid Carbon Nanotube Yarn Muscles," *Science*, vol. 338, no. 6109, pp. 928–932, Nov. 2012.

[3] S. S. Brenner, "Growth and Properties of 'Whiskers' Further research is needed to show why crystal filaments are many times as strong as large crystals," *Science*, vol. 128, no. 3324, pp. 569–575, Sep. 1958.

[4] R. Mehan and J. Herzog, "Whisker," in *Whisker Technology*, A. Levitt, Ed. New York: John Wiley & Sons, 1970, pp. 157–196.

[5] W. W. Webb and W. D. Forgeng, "Mechanical behavior of microcrystals," *Acta Metallurgica*, vol. 6, no. 7, pp. 462–469, Jul. 1958.

[6] M. Salkind, F. Lemkey, and F. George, "Whisker Composites by Eutectic Solidification," in *Whisker Technology*, A. Levitt, Ed. New York: John Wiley & Sons, 1970.

[7] S. S. Brenner, "Plastic Deformation of Copper and Silver Whiskers," *Journal of Applied Physics*, vol. 28, no. 9, pp. 1023 –1026, Sep. 1957.

[8] K. Yoshida, Y. Goto, and M. Yamamoto, "Yielding of Copper Whiskers," *Journal of the Physical Society of Japan*, vol. 21, no. 4, pp. 825–826, 1966.

[9] M.-F. Yu, O. Lourie, M. J. Dyer, K. Moloni, T. F. Kelly, and R. S. Ruoff, "Strength and Breaking Mechanism of Multiwalled Carbon Nanotubes Under Tensile Load," *Science*, vol. 287, no. 5453, pp. 637–640, Jan. 2000.

[10]   C. W. Sinclair, J. D. Embury, G. C. Weatherly, K. T. Conlon, C. P. Luo, and K. Yu-Zhang, "Diffraction based characterization of a directionally solidified Cu–Cr eutectic alloy," *Journal of Crystal Growth*, vol. 276, no. 1–2, pp. 321–331, Mar. 2005.

[11]   J. Bevk, J. P. Harbison, and J. L. Bell, "Anomalous increase in strength of in situ formed Cu #x2010;Nb multifilamentary composites," *Journal of Applied Physics*, vol. 49, no. 12, pp. 6031 –6038, Dec. 1978.

[12]   W. . Spitzig, A. R. Pelton, and F. C. Laabs, "Characterization of the strength and microstructure of heavily cold worked Cu   Nb composites," *Acta Metallurgica*, vol. 35, no. 10, pp. 2427–2442, Oct. 1987.

[13]   K. Han, J. D. Embury, J. R. Sims, L. J. Campbell, H.-J. Schneider-Muntau, V. I. Pantsyrnyi, A. Shikov, A. Nikulin, and A. Vorobieva, "The fabrication, properties and microstructure of Cu–Ag and Cu–Nb composite conductors," *Materials Science and Engineering: A*, vol. 267, no. 1, pp. 99–114, Jul. 1999.

[14]   L. Thilly, F. Lecouturier, G. Coffe, J. P. Peyrade, and S. Askénazy, "Ultra high strength nanofilamentary conductors: the way to reach extreme properties," *Physica B: Condensed Matter*, vol. 294–295, no. 0, pp. 648–652, Jan. 2001.

[15]   M. Zhang, K. R. Atkinson, and R. H. Baughman, "Multifunctional Carbon Nanotube Yarns by Downsizing an Ancient Technology," *Science*, vol. 306, no. 5700, pp. 1358–1361, Nov. 2004.

[16]   J. Foroughi, G. M. Spinks, G. G. Wallace, J. Oh, M. E. Kozlov, S. Fang, T. Mirfakhrai, J. D. W. Madden, M. K. Shin, S. J. Kim, and R. H. Baughman, "Torsional Carbon Nanotube Artificial Muscles," *Science*, vol. 334, no. 6055, pp. 494–497, Oct. 2011.

[17]   J. D. W. Madden, N. A. Vandesteeg, P. A. Anquetil, P. G. A. Madden, A. Takshi, R. Z. Pytel, S. R. Lafontaine, P. A. Wieringa, and I. W. Hunter, "Artificial muscle technology: physical principles and naval prospects," *IEEE Journal of Oceanic Engineering*, vol. 29, no. 3, pp. 706 – 728, Jul. 2004.

[18]   J. M. Hollerbach, I. W. Hunter, and J. Ballantyne, "The robotics review 2," O. Khatib, J. J. Craig, and T. Lozano-Pérez, Eds. Cambridge, MA, USA: MIT Press, 1992, pp. 299–342.

[19]   I. A. Anderson, T. Hale, T. Gisby, T. Inamura, T. McKay, B. O'Brien, S. Walbran, and E. P. Calius, "A thin membrane artificial muscle rotary motor," *Appl. Phys. A*, vol. 98, no. 1, pp. 75–83, Jan. 2010.

[20]   R. H. Baughman, C. Cui, A. A. Zakhidov, Z. Iqbal, J. N. Barisci, G. M. Spinks, G. G. Wallace, A. Mazzoldi, D. D. Rossi, A. G. Rinzler, O. Jaschinski, S. Roth, and M. Kertesz, "Carbon Nanotube Actuators," *Science*, vol. 284, no. 5418, pp. 1340–1344, May 1999.

[21]   T. Mirfakhrai, J. Oh, M. Kozlov, E. C. W. Fok, M. Zhang, S. Fang, R. H. Baughman, and J. D. W. Madden, "Electrochemical actuation of carbon nanotube yarns," *Smart Materials and Structures*, vol. 16, no. 2, pp. S243–S249, Apr. 2007.

[22]   L. Klintberg, M. Karlsson, L. Stenmark, J.-Å. Schweitz, and G. Thornell, "A large stroke, high force paraffin phase transition actuator," *Sensors and Actuators A: Physical*, vol. 96, no. 2–3, pp. 189–195, Feb. 2002.

[23]   J. D. W. Madden, B. Schmid, M. Hechinger, S. R. Lafontaine, P. G. A. Madden, F. S. Hover, R. Kimball, and I. W. Hunter, "Application of polypyrrole actuators: feasibility of variable camber foils," *IEEE Journal of Oceanic Engineering*, vol. 29, no. 3, pp. 738 – 749, Jul. 2004.

[24]   M. Nič, J. Jirát, B. Košata, A. Jenkins, and A. McNaught, Eds., "modulus of elasticity, E," in *IUPAC Compendium of Chemical Terminology*, 2.1.0 ed., Research Triangle Park, NC: IUPAC.

[25]   M. Nič, J. Jirát, B. Košata, A. Jenkins, and A. McNaught, Eds., "shear stress, τ," in *IUPAC Compendium of Chemical Terminology*, 2.1.0 ed., Research Triangle Park, NC: IUPAC.

[26]   M. Nič, J. Jirát, B. Košata, A. Jenkins, and A. McNaught, Eds., "shear strain, γ," in *IUPAC Compendium of Chemical Terminology*, 2.1.0 ed., Research Triangle Park, NC: IUPAC.

[27]   Y. Leprince-Wang, K. Han, Y. Huang, and K. Yu-Zhang, "Microstructure in Cu–Nb microcomposites," *Materials Science and Engineering: A*, vol. 351, no. 1–2, pp. 214–223, Jun. 2003.

[28]   M. Miao, "Electrical conductivity of pure carbon nanotube yarns," *Carbon*, vol. 49, no. 12, pp. 3755–3761, Oct. 2011.

[29]   K. Koziol, J. Vilatela, A. Moisala, M. Motta, P. Cunniff, M. Sennett, and A. Windle, "High-Performance Carbon Nanotube Fiber," *Science*, vol. 318, no. 5858, pp. 1892–1895, Dec. 2007.

[30]   S. M. Mirvakili, A. Pazukha, W. Sikkema, C. W. Sinclair, G. M. Spinks, R. H. Baughman, and J. D. W. Madden, "Niobium Nanowire Yarns and their Application as Artificial Muscles," *Advanced Functional Materials*, p. n/a–n/a, 2013.

APPENDICES

Appendix A: Some math

We can use the helical model for the twisted niobium yarns. The left drawing in Figure A.1 represents the natural state of the twisted yarn and the middle drawing illustrates the twisted niobium yarn after actuation. The yarn is held at one side only; therefore, the length of the yarn shrinks while its diameter increase. From the graph in the right we find

$$\sin(\alpha) = \frac{2n\pi r}{L_s}, \ \cos(\alpha) = \frac{L}{L_s} \tag{A1}$$

$$\alpha = \tan^{-1}\left(\frac{2n\pi r}{L}\right) = \tan^{-1}(2\pi rT) \tag{A2}$$

where T is the number of turns per yarn's length.
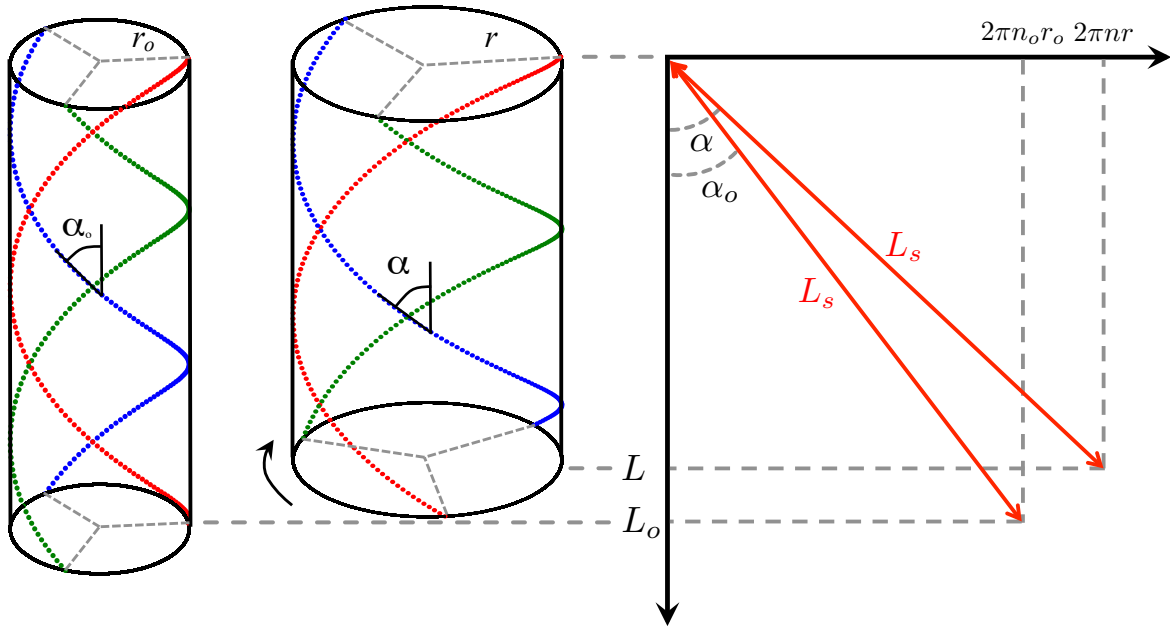
Figure A.1 – Helical Model

Volume of a cylinder can be found by $V = \pi r^2 L$. From equation (A1), we know $r = \frac{L_s \sin(\alpha)}{2\pi n}$ and $L = L_s \cos(\alpha)$. Therefore,

$$V = \frac{L_s^3 \sin^2(\alpha)\cos(\alpha)}{4\pi n^2} \tag{A3}$$

Maximum of the equation (A3) occurs at the maximum of the $sin^2(\alpha)\cos(\alpha)$ which is at $\alpha = 54.736°$ (Figure A.2).
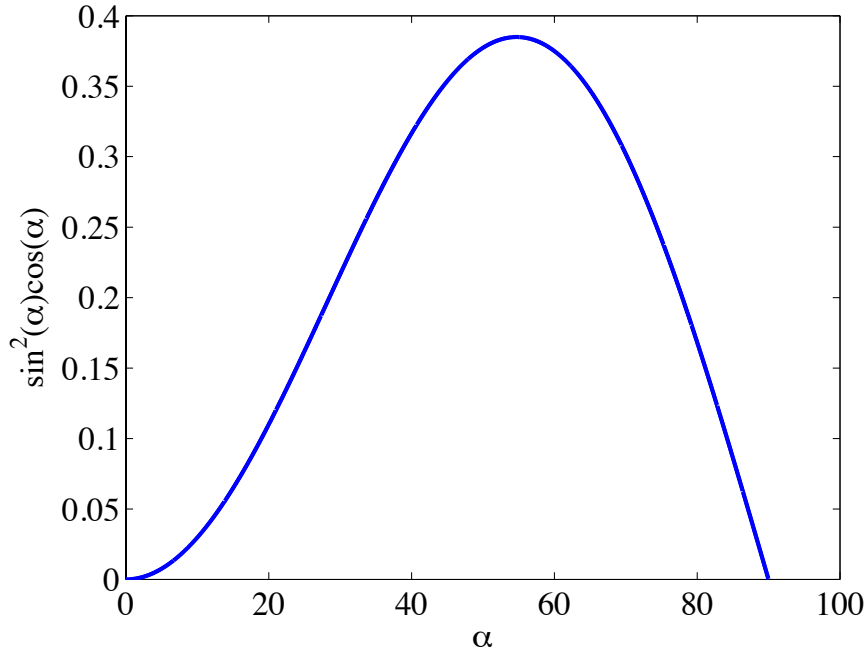

Figure A.2 – Maximum of the volume as a function of twist angle.

Equation (A3) can be written in terms of the fibre length as:

$$V = \frac{L\left(L_s^2 - L^2\right)}{4\pi n^2} \tag{A4}$$

Number of turns (n) would be:

$$n = \sqrt{\frac{L\left(L_s^2 - L^2\right)}{4\pi V}} \tag{A5}$$

This equation also holds for the initial volume (V_o) and initial number of twists (n_o). The ratio would be:

$$\frac{n}{n_o} = \sqrt{\frac{V_o}{V} \cdot \frac{\lambda L_o L_s^2 - \lambda^3 L_o^3}{L_o L_s^2 - L_o^3}} \tag{A6}$$

where λ is the length ratio (L/L_o).

By preventing the yarn from twisting or untwisting (i.e. $n = n_o$) during the actuation, the strain can be found as follow:

$$\frac{n}{n_o} = \sqrt{\frac{V_o}{V} \cdot \frac{\lambda L_o L_s^2 - \lambda^3 L_o^3}{L_o L_s^2 - L_o^3}} = 1 \tag{A7}$$

$$\lambda = \frac{L}{L_o} \Rightarrow \lambda = 1 + \varepsilon \tag{A8}$$

$$\frac{V}{V_o} = \frac{(1+\varepsilon)L_o L_s^2 - (1+3\varepsilon)L_o^3}{L_o L_s^2 - L_o^3} \Rightarrow \varepsilon = \frac{\Delta V}{V_o} \frac{L_s^2 - L_o^2}{L_s^2 - 3L_o^2} \tag{A9}$$

dividing the numerator and denominator by L_o^2 leads to:

$$\varepsilon = \frac{\Delta V}{V_o} \frac{\tan^2(\alpha_o)}{\tan^2(\alpha_o) - 2} \tag{A10}$$

As Figure A.3 and Figure A.4 suggest, as the volume increases, if we keep the length constant, the yarn would untwist. If we prevent the yarn from twisting or untwisting, for low bias angles (below 54.74°) if the volume increases the yarn length decreases and if the angle is above 54.74° the length increases.
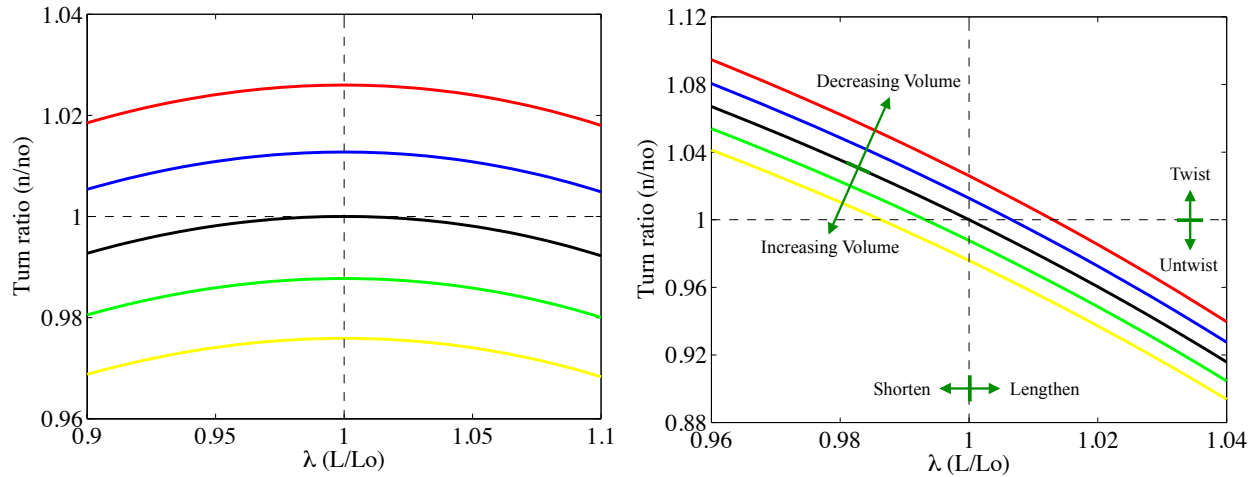
Figure A.3 – The initial yarn bias angle for n/n₀=1 and L/L₀=1 is 54.736° for the left graph and 33° for the graph in the right. Red, blue, black, green, and yellow lines are for yarn volume changes of -5%, -2.5%, 0%, 2.5%, and 5% respectively.
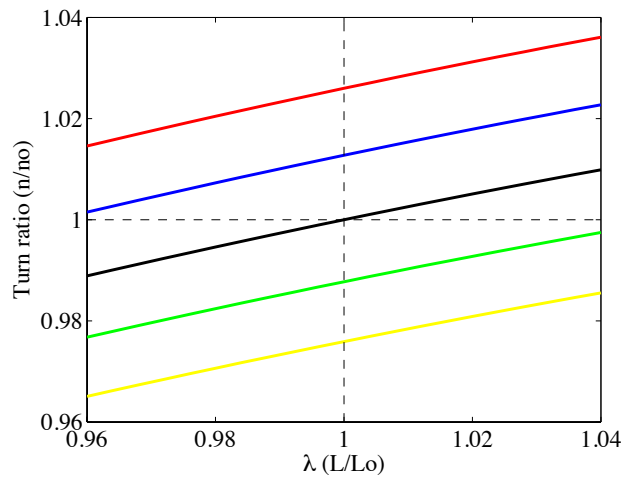

Figure A.4 – In this case the bias angle is 64°. Keeping the yarn from twisting, as the volume increases the yarn length increases as well.

Effect of yarn length on actuation performance:
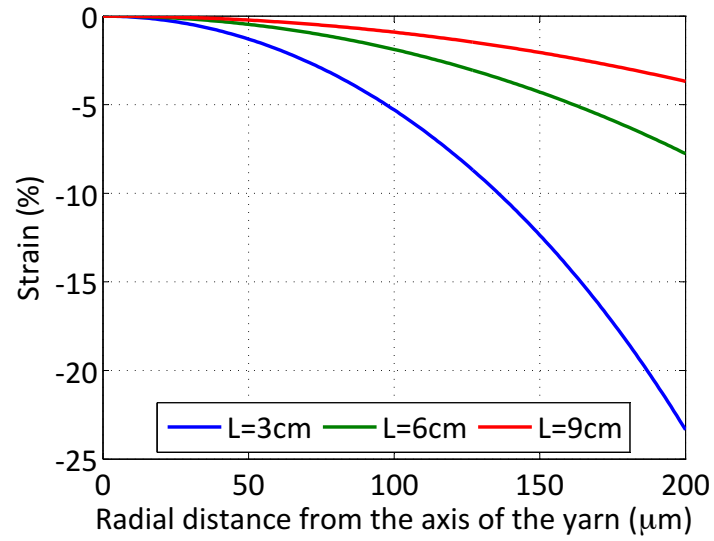
Figure A.5 – Effect of twist on the performance. Number of turns is 20 turns.

As the number of twists increases the fibres at the surface of the yarn break. As Figure A.5 suggests strain on the individual fibres is at its maximum at the surface of the twisted yarn.
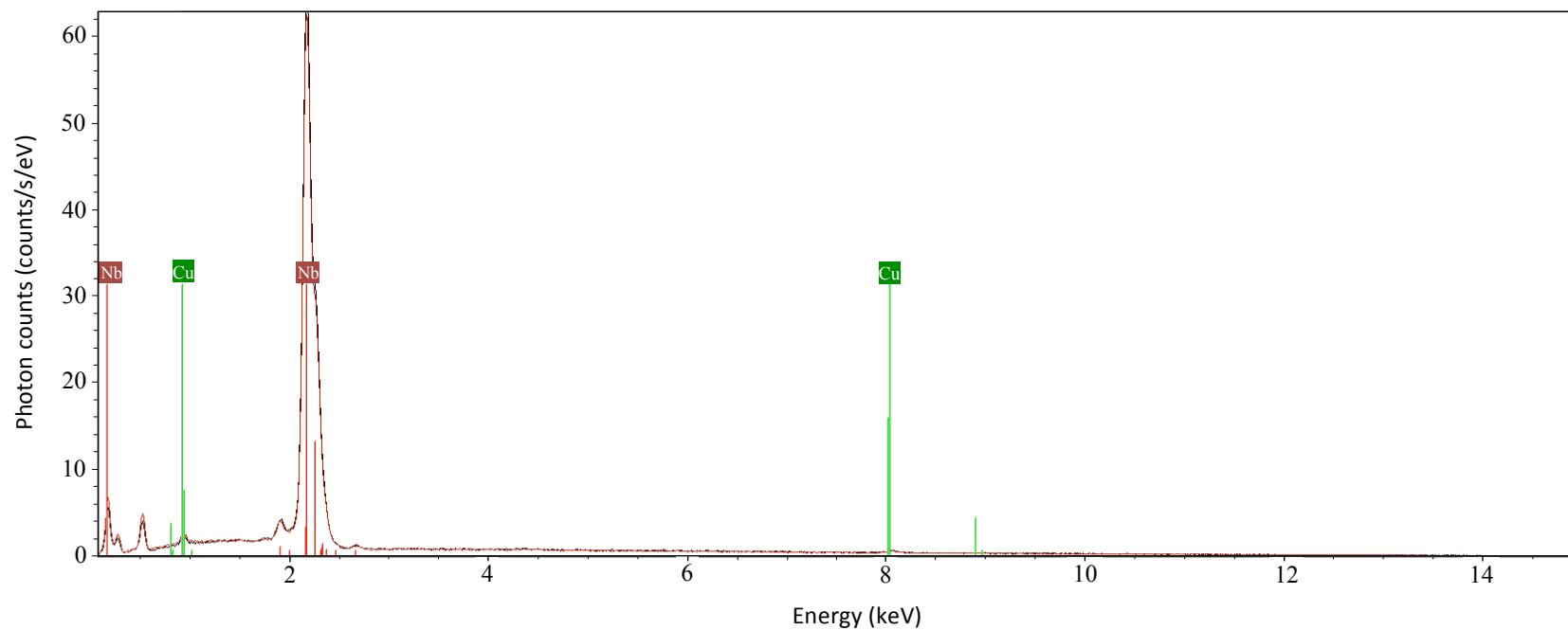
Figure A.6 – Elemental analysis of niobium yarns. Electron-dispersive X-ray spectroscopy with SEM elemental analysis confirms that after the seven-day etching period the nanowire samples consists primarily of niobium, with some copper remaining.
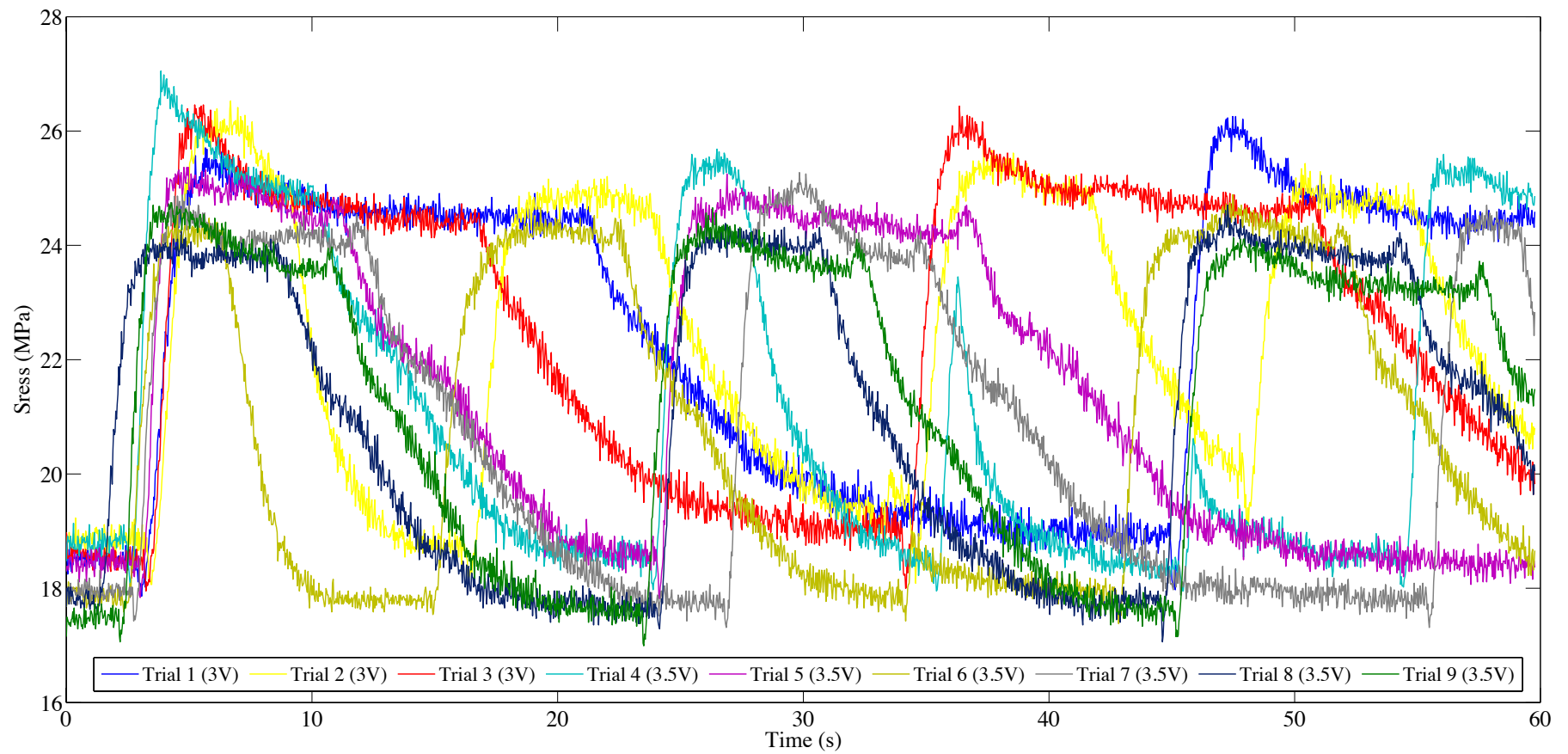
Figure A.7 – 27 cycles of linear actuation in nine trials with applied voltages of 3V and 3.5V. The same yarn as in Figure 4.6 is used.

Table A.1 – Data related to Figure A.7.

|	Trial 1	Trial 2	Trial 3	Trial 4	Trial 5	Trial 6	Trial 7	Trial 8	Trial 9	Avg.	S.D.
Induced stress (MPa)	7.37	5.18	7.59	6.29	7.07	4.33	7.02	6.46	7.02	6.51	1.51
Stress rate (MPa/s)	4.68	3.42	5.63	6.42	5.94	5.38	5.75	5.38	5.38	5.46	0.88
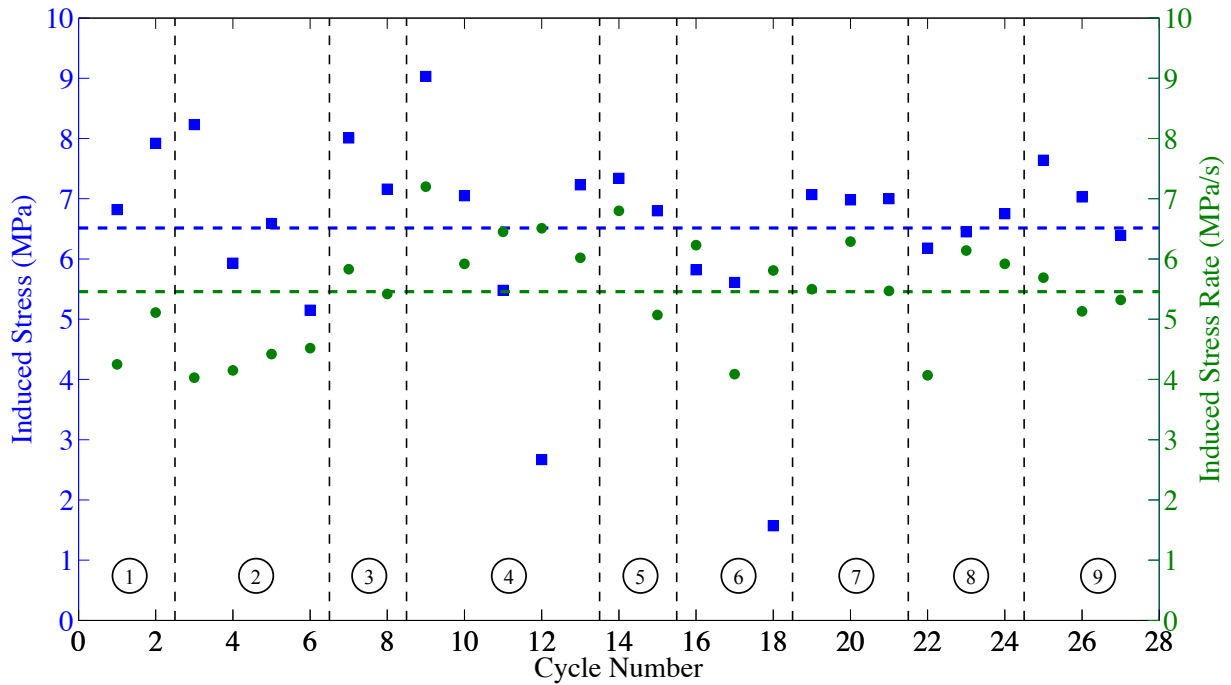
Figure A.8 – Plot of the data related to Figure A.7 and Table A.1. The blue and green horizontal dashed-lines represent the average of the data. Trial numbers are mentioned inside circles.

Table A.2 – Tensile strength vs radius of the yarn

|	Trial 1	Trial 2	Trial 3	Trial 4	Trial 5	Trial 6
Stress (MPa)	1100	68	37	153	560	643
Radius (μm)	7	10.5	9.5	32.5	17.5	25.1
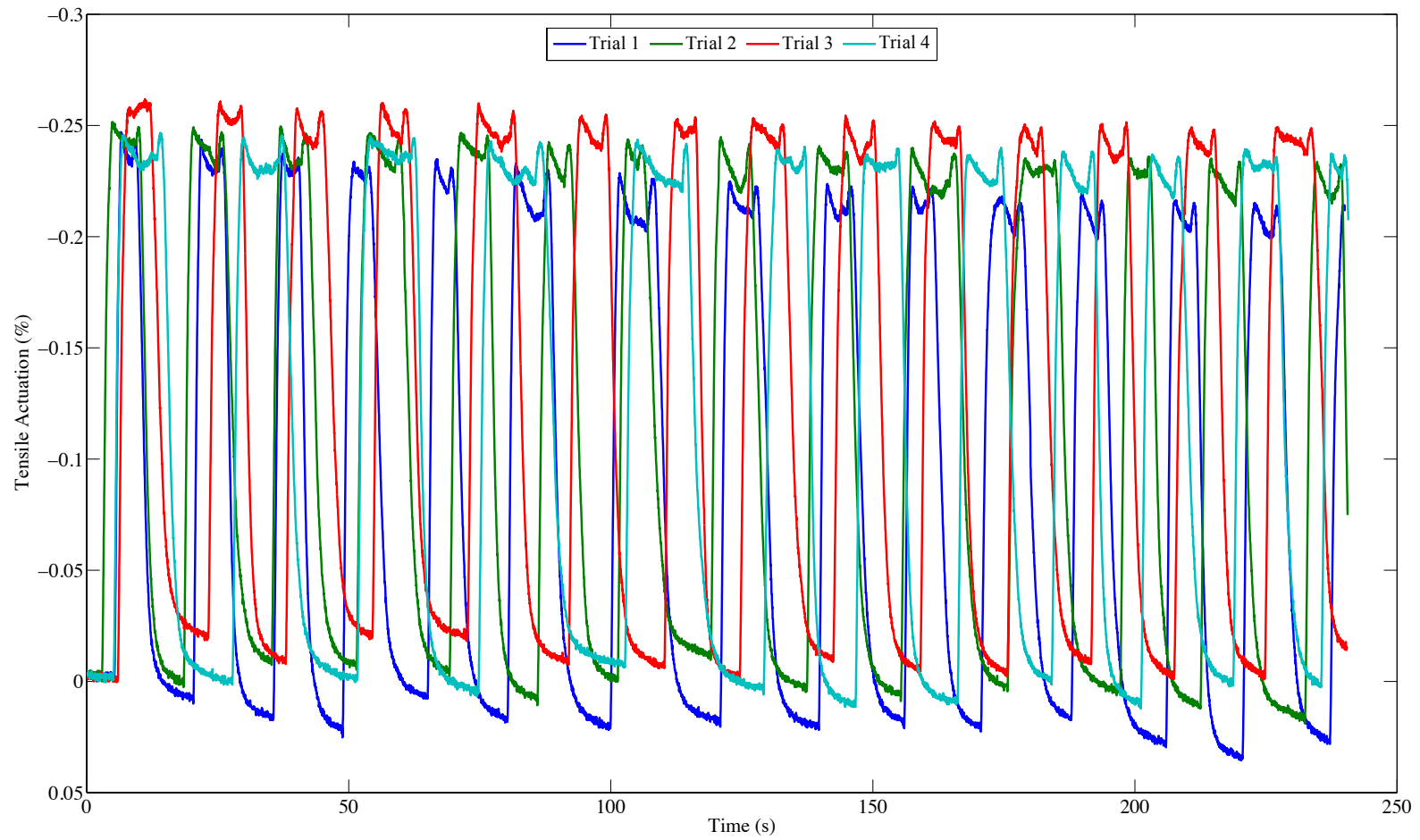
Figure A.9 – Four trials of tensile actuation of the same yarn used in Figure 4.7. The yarn is held at a constant load of 20 MPa.

Appendix C: More images.
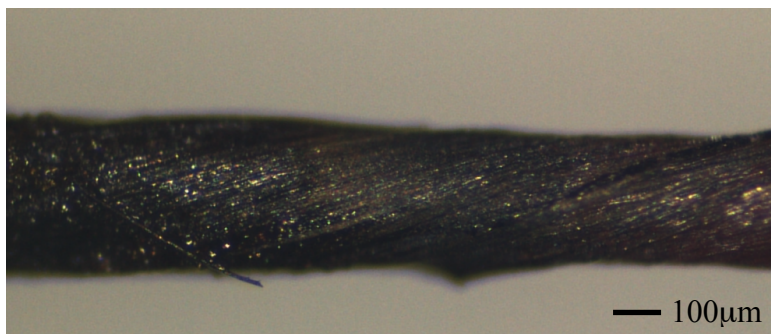
Figure A.10 – The yarn used for IR measurements.